ADNAN SALAH ADNAN ALHAJ OTHMAN

MODELLING OF PV OUTPUT POWER BAS EXPERIMENTAL DATA USING EMPIRI MODELS

MASTER THESIS

2021

NEAR EAST UNIVERSITY

INSTITUTE OF GRADUATE STUDIES

DEPARTMENT OF MECHANICAL ENGINEERING

MODELLING OF PV OUTPUT POWER BASED ON EXPERIMENTAL DATA USING EMPIRICAL MODELS

M.Sc. THESIS

ADNAN SALAH ADNAN ALHAJ OTHMAN

Nicosia

December, 2021

NEAR EAST UNIVERSITY

INSTITUTE OF GRADUATE STUDIES

DEPARTMENT OF MECHANICAL ENGINEERING

MODELLING OF PV OUTPUT POWER BASED ON EXPERIMENTAL DATA USING EMPIRICAL MODELS

M.Sc. THESIS

ADNAN SALAH ADNAN ALHAJ OTHMAN

Supervisor

Assoc. Prof. Dr. Youssef KASSEM

Nicosia

December, 2021

Approval

We certify that we have read the thesis submitted by ADNAN ALHAJ OTHMAN, **"(MODELLING OF PV OUTPUT POWER BASED ON EXPERIMENTAL DATA USING EMPIRICAL MODELS)**" and that in our combined opinion it is fully adequate, in scope and in quality, as a thesis for the degree of Master of Educational Sciences.

Examining Committee	Adnan Salah Adnan Alhaj Othman	Signature
Head of the Committee: Prof. Dr.Adil AMİRJANOV		……
Committee Member*: Assoc. Prof. Dr. Hüseyin ÇAMUR		……
Supervisor: Assoc. Prof. Dr. Youssef KASSEM		……
Approved by the Head of the Department		

16/12/2021

……..

Assoc. Prof. Dr. Hüseyin ÇAMUR

Head of Department

Approved by the Institute of Graduate Studies

…../…../20…

Prof. Dr. Kemal Hüsnü Can Başer

Head of the Institute

Declaration

I hereby declare that all information, documents, analysis and results in this thesis have been collected and presented according to the academic rules and ethical guidelines of Institute of Graduate Studies, Near East University. I also declare that as required by these rules and conduct, I have fully cited and referenced information and data that are not original to this study.

Adnan Salah Adnan Alhaj Othman

16/12/2021

Acknowledgments

I would like to thank my supervisor, Assoc. For his patience, guidance, and support, Prof. Dr. Youssef KASSEM. I have benefited greatly from your wealth of knowledge and meticulous editing. I am extremely grateful that you took me on as a student and continued to believe in me through the years.

I am grateful to Prof. Dr. Hüseyin ÇAMUR. He provided thoughtful feedback, which has been a source of encouragement to me. My sincere thanks are owed out to the interviewees who took time out of their busy schedules to contribute to my research.My parents have been a great support to me throughout my life. They never fail to stand by me no matter what. Mom, thanks for fielding a ridiculous number of phone calls, for calming me down, and for proofreading anytime, anywhere. Dad, thanks for all of your love and for always reminding me of the end goal.

Thanks to my sisters, also, in this achievement, I would like to thanks all of you very much for what you have given me.

Thanks to research colleagues, Mohamedalmojtba Hamid Ali ABDALLA, thanks for continually listening to me rant and talk, for proofreading time and time again (even after long days at work and during difficult times), for cracking jokes when things got too serious, and for your sacrifices that helped me pursue a Master's degree.

Adnan Salah Adnan Alhaj Othman

Abstract

Modelling of PV Output Power Based on Experimental Data Using Empirical Models

MA, Department of Mechanical Engineering (December), (2021), (85) pages

Predicting the photovoltaic (PV) output power is an essential for the secure, stable and economic operation of power grid. Hence, identification of the most relevant parameters that influenced the PV output power is an important task to achieve accurate predictions. This paper presents a comparative study between an empirical equation (Quadratic model (QM)), Multilayer Feed-Forward Neural Network (MFFNN), Cascade Feed-forward Neural Network (CFNN), Radial Basis Neural Network (RBNN), and Elman neural network (ENN)) and multiple linear regression (MLR) for modelling daily PV output power (PV-output) of 68kW grid-connected rooftop solar system located in Amman, Jordan. 57 models with various combinations of parameters including (Day (D), relative humidity (RH), average temperature (AT), maximum temperature (Tmax), minimum temperature (Tmin), wet-bulb temperature (Tw), wind speed (WS) and global solar radiation (GSR)) were proposed to identify most influencing input parameters for predicting the PV output power. The coefficient of determination and root mean squared error were used to select the best predictive model. For this purpose, the meteorological parameters including average temperature, minimum and maximum temperatures, wet-bulb temperature, relative humidity, global solar radiation, and wind speed were measured using weather-monitoring device. Furthermore, the PV output power of 68kW grid-connected PV system was measured using data logger. The data set covers 12 operating months (01 January-31 December 2020). The collected actual data indicate that the maximum value of PV output of 451.25 MWh occurred in May and the minimum value of 32.83 MWh is recorded in January. Out of the 57 machine learning models, The ENN#24, ENN#56, CFNN#12 and CFNN#57 with the combination of [Tw, GSR], [D, Ta, Tmax, Tmin, Tw, GSR, RH], [Ta, GSR], and [D, Ta, Tmax, Tmin, Tw, GSR, WS, RH], respectively, have shown the best prediction. The most significant input parameter for forecasting the PV-output are found to be wet-bulb temperature, global solar radiation and average temperature. In the end, the findings demonstrated that the ENN and CFNN models performed well and presented high accuracy in estimating the value of PV output power.

***Key Words**:* Quadratic model; artificial intelligence models; Multiple linear regressions; meteorological parameters, PV output power; Amman; Jordan

Abstract

Modelling of PV Output Power Based on Experimental Data Using Empirical Models

Adnan Salah Adnan Alhaj Othman

MA, Department of Mechanical

Engineering (December), (2021), (85) pages

***Keywords**:* Quadratic model; artificial intelligence models; Multiple linear regressions; meteorological parameters, PV output power; Amman; Jordan.

Table of Contents

Page

CHAPTER IV

CHAPTER V

List of Tables

List of Figure

List of Abbreviations

PV:	photovoltaic
QM:	Quadratic Model
MFFNN:	Multilayer Feed-Forward Neural Network
CFNN:	Cascade Feed-Forward Neural Network
RBNN:	Radial Basis Neural Network
ENN:	Elman Neural Network
MLR:	Multiple Linear Regression
D:	Day
RH:	Relative Humidity
TA:	Average Temperature
Tmax:	Maximum Temperature
Tmin:	Minimum Temperature
TW:	Wet-Bulb Temperature
WS:	Wind Speed
GSR:	Global Solar Radiation
SD:	Standard Deviation
CV:	Coefficient of Variation
ML:	Machine Learning
AI:	Artificial Intelligence
MSE:	Mean squared error
RMSE:	Root Mean squared error

CHAPTER I

Introduction

This chapter contains information about the research's origins, aim, and limitations.

Background

Humanity has always relied on energy. Until recently, traditional fossil fuels were sufficient to meet this need Nevertheless, fossil fuel consumption has degraded the environment and caused climate change because it emits greenhouse gases (Riahi et al. 2017). Because of the environmental issues associated with greenhouse gas emissions, which have resulted in increased usage of fossil fuels, scientific experts have supported the development of alternative energy sources that can both create energy and safeguard the environment (Vijayavenkataraman et al. 2012; Researchers have discovered that renewable energy sources, such as solar and wind, can significantly reduce greenhouse gas emissions. A requirement for zero-emission manufacturing is solar thermal energy, as suggested by Schnitzer et al. (2007). The role of renewable energies in future energy supply and reduction of greenhouse gas emissions is well documented by Shahsavari and Akbari (2018). Iran's ecology may benefit from the use of solar energy, according to Shahsavari et al. (2018).

In a recent report, solar energy was named as a promising, economically feasible, and environmentally friendly renewable energy source. There have been a number of studies looking at the feasibility of converting solar energy into electricity all around the world. For instance, Adnan et al. (2012) assessed Pakistan's solar energy potential by measuring weather data from fifty-eight meteorological stations across Pakistan. A 100-square-meter plot of land can generate 45 MW to 83 MW of power every month in the southern Punjab, Sindh, and Baluchistan areas. Using wind and solar energy as sources of energy for a small home, Kassem et al. (2019) investigated the possibilities in three northern Cyprus metropolitan areas. These cities have large potential Potential of solar energy vs. potential of wind energy the viability of a 12MW grid-connected wind/PV project in two Northern Cyprus districts was investigated by Kassem et al. (2018). Comparison to wind energy, the results showed that the chosen places had a lot of potential. Enongene et al. (2019) conducted a techno-economic analysis of a small-scale PV system in n residential structures in Nigeria's Lagos

Metropolitan Area. According to the findings, the suggested approach has the potential to help Nigeria meet its GHG reduction goals.

Purpose of the Study

Energy has been a vital requirement for humans. Until recently, traditional fossil fuels were able to meet this need. However, because of greenhouse gas emissions, the usage Climate change has been worsened by the over-use of fossil fuels (Riahi et al. 2017). Due to environmental concerns over greenhouse gas emissions, which have resulted in significant usage of fossil fuels, scientists have pushed the development of alternative energy sources that can both create energy and protect the environment (Vijayavenkataraman et al. 2012; Arreyndip and Joseph 2018). Many scientific studies have discovered that green solar reduced carbon dioxide emissions (GHG) are achieved in part through energy and wind. Solar thermal energy was found to be an essential step toward achieving zero-emission manufacturing by Schnitzer et al. (2007), for instance. A growing part of future energy expansion can be implemented through renewable energy sources, assert Shahsavari and Akbari (2018). Iran's eco-system may benefit from producing power through the use of solar systems, based on Shahsavari et al. (2018). Predicting the photovoltaic (PV) output power is an essential for the secure, stable and economic operation of power grid. Hence, identification of the most relevant parameters that influenced the PV output power is an important task to achieve accurate predictions. This paper presents a comparative study between an empirical equation (Quadratic model (QM)), Multilayer Feed-Forward Neural Network (MFFNN), Cascade Feed-forward Neural Network (CFNN), Radial Basis Neural Network (RBNN), and Elman neural network (ENN)) and multiple linear regression (MLR) for modelling daily PV output power (PV-output) of 68kW grid-connected rooftop solar system located in Amman, Jordan. 57 models with various combinations of parameters including (Day (D), relative humidity (RH), average temperature (AT), maximum temperature (Tmax), minimum temperature (Tmin), wet-bulb temperature (Tw), wind speed (WS) and global solar radiation (GSR)) were proposed to identify most influencing input parameters for predicting the PV output power. The coefficient of determination and root mean squared error were used to select the best predictive model. For this purpose, the meteorological parameters including average temperature, minimum and maximum temperatures, wet-bulb temperature, relative

humidity, global solar radiation, and wind speed were measured using weather-monitoring device. Furthermore, the PV output power of 68kW grid-connected PV system was measured using data logger. The data set covers 12 operating months (01 January-31 December 2020). The collected actual data indicate that the maximum value of PV output of 451.25 MWh occurred in May and the minimum value of 32.83 MWh is recorded in January. Out of the 57 machine learning models, The ENN#24, ENN#56, CFNN#12 and CFNN#57 with the combination of [Tw, GSR], [D, Ta, Tmax, Tmin, Tw, GSR, RH], [Ta, GSR], and [D, Ta, Tmax, Tmin, Tw, GSR, WS, RH], respectively, have shown the best prediction. The most significant input parameter for forecasting the PV-output are found to be wet-bulb temperature, global solar radiation and average temperature. In the end, the findings demonstrated that the ENN and CFNN models performed well and presented high accuracy in estimating the value of PV output power.

Recent research indicates solar energy is one of the most effective, environmentally friendly, and economically viable sources of renewable energy. Solar energy has been the subject of several studies looking at the possibility of generating electricity from it in various parts of the world. A study by Adnan et al. (2012), for instance, evaluated the potential of solar power in Pakistan by using fifty-eight meteorological stations. An area of 100 m2 in southern Punjab, Sindh, and Pakistan could generate 45 MW to 83 MW of power each month, according to the findings. This could be applied to the Baluchistan regions as well. According to Kassem et al. (2019), they investigated whether wind and solar energy can be used for a small home in three metropolitan areas in Northern Cyprus. The selected locations showed a much greater potential for solar energy than windy environments. Researchers from Kassem et al. (2018) examined two districts of Northern Cyprus.

An investigation was carried out into the feasibility of a grid-connected 12MW wind/PV plant. The results showed that the selected places have a very high potential for wind energy compared with wind power. According to Enongene et al. (2019), residential buildings in Lagos Metropolitan Area, Nigeria, are equipped with small-scale PV systems.The findings revealed that the suggested approach has the potential to help Nigeria meet its GHG reduction objectives.

CHAPTER II

Jordan

This chapter provides research-related conceptual definitions, descriptions, and information on the subject that already exists in the literature.

Jordan

There are 89,342 km2 of territory in Jordan's Hashemite Kingdom (HKJ) on the northern Arabian Peninsula. In addition to Palestine, Iraq, Syria, and Saudi Arabia, it shares borders with them all. In most of the country, only about a quarter can be cultivated. In summer, Jordan has a semiarid climate while in winter, it has a frigid climate. Across all industries, Jordan has seen a steady rise in consumption of 4–5% annually over the past few years. Electricity usage in 2018 was 17,439 GWh, with a peak load of 3,100 GWh. Furthermore, home consumption accounted for 45.12 percent, with industry (22.07 percent), water pumping, and commercial accounting rounding out the top five (15 percent). Jordan needs to import 7,656 ktoe (thousand tonnes of oil equivalent) of energy to satisfy its needs due to native supplies. As a result, Jordan has two major challenges: the first is growing energy consumption, and the second is a scarcity of local resources. This makes meeting the country's demands difficult.

Jordan's government has set a goal of using renewable energy sources such as wind and solar energy to meet 10% of its energy demands. By 2020, the majority of this will be accomplished by expanding renewable power output from 1.13 GW to 1.8 GW.

Wind speeds in Jordan range from 7 to 11 m/s, which are ideal for producing energy. In comparison to other sections of the country, the southern and northern parts of the country have the greatest wind energy potential. At 1996, the German Eldorado program built the first wind farm in Hofa, which has a capacity of 1.125MW. The second wind farm, with a capacity of 320 kW and funded by a Dutch business, was established in 1998 at Brahimyya. Ma'an hosts the third wind farm, which has a capacity of 66MW (southeast of Jordan). In general, the quantity of power generated by wind energy is predicted to rise from 600MW to 1000MW between 2019 and 2021.Moreover, Jordon seems to have an average of 310 bright days per year with direct solar radiation intensity ranging from 5kWh/m2 to

7kWh/m2. Furthermore, yearly direct sun radiation levels range from 1800 to 2700 kWh/m2. Furthermore, the daily average of horizontal solar radiation is around 5.6 kWh/m2. Solar energy will create around 800MW of power in 2020. In 2015, twelve direct Power Purchase Ma'an Development Area has signed PPAs for building and generating 200 MW of electricity. One more solar power plant in the Quweirah area (Aqaba) has been sponsored by Gulf Corporation Council Fund. which is now being assessed. Capacity ranges from 75 to 100 megawatts. Solar water heaters are installed on the roofs of nearly 20% of Jordanian homes. By 2020, solar water heating systems will be used in 30% of all residences, according to the Energy Master Plan. Installed on roofs are solar water heater panels covering 1.40 km2 and a PV system generating 150 kWh of electricity. Over 4500 solar water heaters are produced annually by 25 small solar water heater manufacturers in the area. There are three windmills with a combined capacity of 125 to 150 MW in the government's proposal, along with hybrid CSPs with a combined capacity of 100 to 250 MW.

Jordan has conducted scientific research into the potential of solar and wind energy in a variety of regions (Anagreh et al. 2010; Alzoubi and Alshboul 2010; Badran et al. 2010, Al-Salaymeh et al. 2010a; Al-Salaymeh et al. 2010b; Anagreh and Bataineh 2011; Al Alawin et al. 2012; El-Tous et al. 2012; Zyadin et al. 2012; Abu-Shikhah et al. 2012; Aagreh and Al-Ghzawi 2013; Alsaad 2013; Fasfous et al. 2013; Sakhrieh and Al-Ghandoor 2013; Al-Sayed 2013; Bataineh et al. 2014; Qasaimeh et al. 2014; Al-Soud and Alsafasfeh 2015; Jaber et al. 2015; Al-Nhoud and Al-Smairan 2015; Ammari et al. 2015; Tashtoush et al. 2015; Khasawneh et al. 2015; Altarawneh et al. 2016; Al-Najideen and Alrwashdeh 2017; Okonkwo et al. 2017; Jaber et al. 2017; Dalabeeh 2017; Al-Ghussain et al. 2017; Alomari et al. 2018; Al-Ghussain et al. 2018; Ayadi et al. 2018; Hammad et al. 2018; Alrwashdeh 2018a, Alrwashdeh 2018b; Alkhalidi et al. 2018; Al-omary et al. 2018; Alrwashdeh 2018c; Alrwashdeh 2018d; Al Safely and Harb 2018; Alrwashdeh and FMA 2018; Alrwashdeh 2018e; Alrwashdeh 2018f; Al-Ghriybah et al. 2019; Abujubbeh et al. 2019; Al-Smairan and Al-Nhoud 2019; Alrwashdeh 2019; Pastor et al. 2020; Al-Addous et al. 2020; Alkhalidi et al. 2020; Al-Addous et al. 2020; Abu-Rumman et al. 2020). For instance, Badran et al. (2010) found that the PV system was considered to be the better option for power generation in the Amman region. Aagreh and Al-Ghzawi (2013) In Ajloun city, Jordan, the on-grid/small wind

turbines and off-grid PV systems proved to be the best energy resources for feeding the hotel's demand. Al-Najideen and Alrwashdeh (2017) assessed that a grid-tied PV system installed at Mu'tah University in Al-Karak region covered the energy demand for the Engineering Faculty with a 56.7kW system.

The solar PV systems identified by Al-Soud and Alsafasfeh (2015) are deemed suitable for generating electricity in the rural areas of Jordan. From previous studies. Figure 2.1 Show Map Solar of Jordan According to previous scientific studies, it can be concluded that:

- Using solar energy in Jordan can help the country generate electricity and become less reliant on fossil resources.
- PV systems have the ability to reduce fossil fuel burning and greenhouse gas emissions, particularly CO2.
- Renewable energy technologies, particularly photovoltaic systems, assist to fulfill the country's rising energy demand.
- PV systems produce more electricity in certain areas and are more suited for small-scale power generation.

Figure 2.1

Map Solar of Jordan

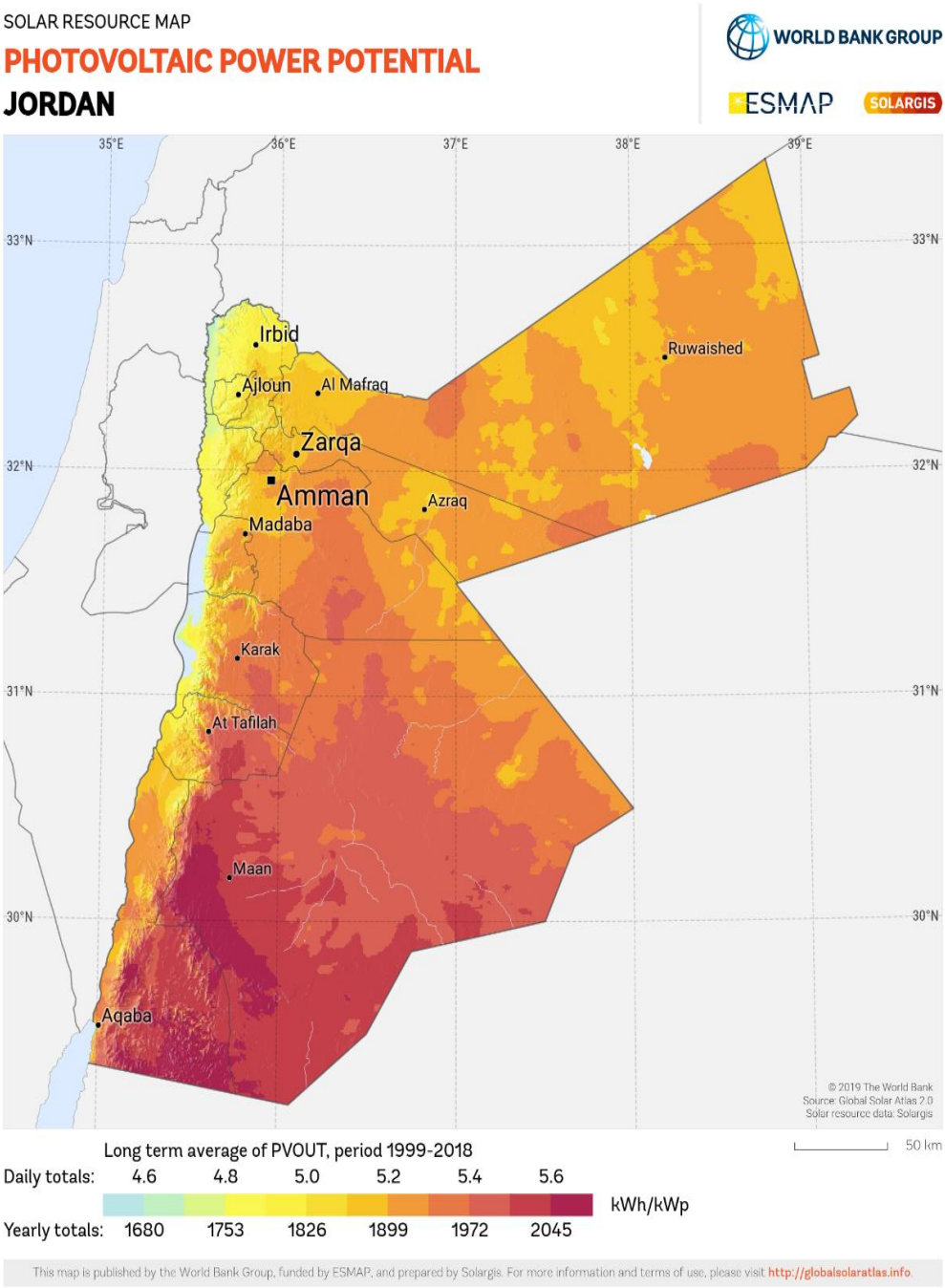

Jordan climate

Jordan has a relatively hot, dry climate, with short, cold winters and long warm, dry summers. Due to its geographic location between the Arabian Desert and the eastern Mediterranean, Jordan's climate is influenced by subtropical aridity. In January, temperatures range between 5 and 10 degrees Celsius, while in August, temperatures range between 20 and 35 degrees Celsius. Temperatures can reach 40°C or more on some days, especially when the Shirocco, a hot, dry southerly breeze, blows. Sandstorms can occur when these winds become very strong. Between November and March, the nation receives over 70% of its annual rainfall; June through August are frequently dry. Rainfall fluctuates from year to year and season to season. During intense storms, precipitation is typically concentrated, producing erosion and local floods, especially in low-lying areas.

Between November and March, the nation receives over 70% of its annual rainfall; June through August are frequently dry. Rainfall fluctuates from year to year and season to season. During intense storms, precipitation is typically concentrated, producing erosion and local floods, especially in low-lying areas.

Energy situations in Jordan

Jordan's energy consumption has been increasing as a result of two factors: economic growth in various industries and an increase in the number of refugees fleeing regional conflict from neighboring countries. The national energy expense, which accounted for 20% of the state budget in 2015, was reduced to 10% in 2018 due to the deployment of energy-saving measures and an increase in the contribution of renewables to the national energy mix. Jordan implemented National Energy Efficiency Action Plans (NEEAPs) in 2012, with the goal of reducing primary power consumption by 20% by 2020.

Growing energy consumption and limited local resources to meet the country's demands are two main difficulties for the oil and gas sector. For example, in 2018, local energy output was 790 ktoe, with natural gas, renewable energy, and to a lesser extent crude oil accounting for the majority of it (representing 7.8 percent of the national energy demand of 9,712 ktoe). Jordan's main energy sources for 2018 are depicted in Figure 1. Imported oil and natural gas supply 87 GW of solar energy

(9,712 ktoe), with domestic sources providing for 7.8% of overall energy supply, with renewables accounting for 7%.

Jordan's electricity output is steadily increasing, paving the opportunity for foreign investment to supply the money and capacity needed to meet the expanding demand. Electricity output reached 5,236.4 megawatts (MW) in 2018 and is predicted to reach 5,770 meters by 2020, highlighting the importance of deploying dependable and clean energy options for the country's socio-economic development.

Transportation accounted for 49% of national power consumption, with home needs accounting for 21.5 cents (lighting, cooling, and heating), the industrial sector accounting for 14%, and agriculture and forestry contributing for 15.5 percent. All gasoline subsidies were phased out by 2012, and power subsidies were phased out in 2017. In 2018, Jordan had to import 8,922 ktoe of energy, which cost the country 10% of its GDP. Egypt was the most significant natural gas supplier because of its large discounts. Regrettably, this supply were cut off, putting Jordan's energy security in jeopardy. Jordan started looking for secure alternatives to renewable resources as a result of the region's unstable political situation. This will provide the state financial weight in procuring low-priced gas from a variety of sources, albeit the political cost is unknown.

Renewable energy in Jordan

Considering the large number of refugees, the expanding residential and retail sectors, and the higher costs of imported fuel and GHG emissions, the country's decision-makers have prioritized a clean, sustainable, and competitive power system. Government officials focused on establishing energy efficiency measures and tracking progress on renewable energy.

Renewable Energy and Energy Efficiency Law (REEL) No. 13 was approved by the government in 2012 to help meet its environmental objectives. Services and industries, which consume the most energy, are covered by energy management and efficiency measures. Through the Jordan Investment Commission, a "one-stop-shop" office is being established to expedite the licensing process for new renewable energy projects to promote new investment. Concerned over energy

production and import costs, the government developed the National Energy Strategy Plan.

Government and EU plans to invest $ 20 billion in energy development by 2020, with a primary focus on renewable energy. The country has recently cut back on nuclear power because of public protests and budget constraints. Oil shale development and renewable energy are also priority efforts.

As a result of this strategy, the percentage of electricity generated from renewable sources will increase from 7% in 2018 to 10% in 2020. Direct investment will create 2,000 MW of wind and solar energy by 2020, according to the National Energy Strategy Plan. A wind farm of 117 MW went online near Al-Tafileh in 2015, and a solar farm of 200 MW was completed in Ma'an in 2016.

Wind and solar energy are two viable renewable energy sources for generating power in the nation. According to a Bloomberg survey from 2017, Jordan ranked first in the Middle East and North Africa (MENA) region for renewable energy adoption and clean energy growth, as well as third globally.

The research, which was founded on the evolution of Jordan's renewable and Investment plans and laws in the renewable energy industry were highlighted. It also looked at the amount of investment that has been made and is expected to be made in the country, as well as the impact of these activities on carbon emission reduction sources. Jordan's trademark in the quest of clean power has been the building of prototype and demonstrator facilities as well as continual investigation of technical advancements in renewable industries. In addition, the electrical regulatory commission published the "Reference Price List" in full disclosure to encourage investment in renewable energy projects and to safeguard investors. Investors can now examine the viability and potential profitability of their project with less risk, which encourages them to invest in renewable energy.

Table 2.1 in the "Benchmark Price List" displays the predicted pricing (Tariff) for renewable energy-generated power. Investors can evaluate their planned investment in renewable energy sources using the "Reference Price List" as the Feed-in Tariff. Developers can bid below this maximum since the winning bidder will receive an additional 15% tariff if they install a 100% local renewable energy source. This will benefit the country's renewable energy companies by encouraging technology transfer.On behalf of Jordanian authorities, the National Electricity Power Company (NEPCO) signed twelve Power Purchase Agreements (PPAs) with

developers to contribute 200 MW of solar energy to the national grid through direct proposal submission. The Church for Energy and Natural Resources (MEMR) has begun Phase II of direct proposal submissions to encourage foreign investment in renewable energy, with the goal of adding 650 MW of wind and solar electricity to the grid. In the second phase, thirteen investors will be chosen to give each developer with 50 megawatts of electricity. The MEMR received financial bids from twenty-three firms for the initial review and negotiation. a brief overview

Table 2.1

Tariff (reference price list) to Renewable Sources.

Resource	**Cents/KWh**
Thermal Solar Energy (CSP)	20
PV	15
Biomass	13
Wind Energy	11
Biogas	9

Importance of the study

It is becoming increasingly critical for PV plants to improve the precision of their power generation predictions in order to improve their penetration into the electrical grid. Energy budgets are particularly affected by solar radiation and the number of clear, sunny days (Mehmood et al. 2014; Khandelwal and Shrivastava 2017). Several researchers have investigated the impact of various input variables on solar radiation forecasts, evaluated their impact on accuracy, and then concluded which are the most useful. The results of this investigation are summarized in Table S1. Other related studies are outlined here.

Empirical methods, including machine learning algorithms and mathematical formulae, are used to estimate PV power output and global solar radiation. Sunlight hours, maximum temperature, lowest temperature, wind speed, rainfall, dew point temperature, relative humidity, cloud cover, and pressure are some of the typical meteorological characteristics used for assessing solar radiation, according to the literature study. According to the authors' review, one research

(Lopes et al. 2020) employed dew point temperature as an input variable for the machine-learning model. Furthermore, it demonstrates a distinct lack of ability in Jordan to anticipate the output power of PV systems. According to our knowledge, no comprehensive studies have been conducted in Jordan that forecast daily PV system output power using average temperatures, minimum and maximum temperatures, wet-bulb temperatures, relative humidity, global solar radiation, and wind speed as inputs.As a result, the goal of this article is to look at the impact of meteorological conditions on PV system output power. Five empirical models (Quadratic model (QM), Multilayer Feed-Forward Neural Network (MFFNN), Cascade Feed-Forward Neural Network (CFNN), Radial Basis Neural Network (RBNN), and Elman neural network (ENN)) and multiple linear regression (MLR) are used to identify the most relevant parameters for daily PV-output power prediction in PV systems.

A weather-monitoring system was used to measure meteorological data such as average temperature, minimum and maximum temperatures, Wet-bulb temperature, relative humidity, global sun radiation, and wind speed. Furthermore, data loggers were used to assess the PV output power of a 68kW grid-connected PV system erected on a flat building section in Amman, Jordan.

Table 2.2

Input Variables Used in Empirical Models Based Prediction of Solar Radiation and Output Power of PV System

References	country	Model	Input	Output
Egeonu et al (2015)	Nigeria	Artificial neural network	sunshine hours, maximum temperature, relative humidity and cloud cover as network inputs	Global Solar Radiation
Worki et al (2016)	Ethiopia	Backward Propagation Artificial Neural Network	Daily average relative humidity, Daily Maximum Temperature, Daily Minimum Temperature, Daily sunshine, Daily wind speed	Global Solar Radiation
Ogliari et al (2017)	Italy	Artificial neural network	Ambient temperature, Global Horizontal Solar irradiance, Plane Of Array total solar irradiance, wind speed, wind direction, pressure, and precipitation.	Electricity power
Safaripourand and Mehrabian (2011)	Iran	Page model equations and Bird-Hulstrom model equations	solar constant, zenith angle, surface pressure, ground albedo, perceptible water vapor, total ozone, and broadband turbidity	Global solar radiation
Rezrazi et al (2016)	Algeria	Artificial neural networks	Direct normal radiation, diffuse radiation (90°), global radiation (90°), global radiation (30°)	Direct normal radiation
An et al (2020)	China	Artificial neural network	Direct normal solar irradiance	Global solar radiation
Lopes et al (2020)	Ireland	Random Forest and multiple linear regression	Dew point temperature, humidity level, visibility, air pressure, wind speed	Global horizontal irradiation

Table 2.2 (Continued)

References	country	Model	Input	Output
Alizamir et al (2020)	Turkey and USA	Multilayer perceptron neural network. Adaptive neuro-fuzzy inference systems. Multivariate adaptive regression spline.	Wind speed, maximum air temperature, minimum air temperature and relative humidity	Global solar radiation
Boubaker et al (2020).	Hail KSA	Feed-Forward Artificial Neural Networks	Temperature, radiation and humidity	Global horizontal irradiation
Guijo-Rubio et al (2020)	Spain	Artificial neural networks	Solar radiation	Global solar radiation Physical model
Guermoui et al (2020)	Italy	Artificial neural networks	Temperature , Relative humidity, Wind speed	Global solar radiation
Kosovic et al (2020)	China	Computational fluid dynamics	Daily average relative humidity, Daily Maximum temperature, Daily Minimum. Temperature, Daily sunshine, Daily wind speed	Solar radiation
Demircan et al (2020)	Turkey	Artificial Bee Colony	Air temperature and relative humidity	Global solar radiation
Polo et al (2020)	Spain	Reanalysis	Atmospheric composition, cloud properties	solar radiation
Tymvios et al (2005)	Cyprus	Artificial neural networks	Daily maximum and minimum temperatures	Global solar radiation
Bosch el at (2008)	India	Artificial neural networks	Relative humidity, Ambient air temperature, Inlet air temperature, Mean air temperature Plate.	Thermal efficiency

Table 2.2 (Continued)

References	country	Model	Input	Output
Linares-Rodríguez et al (2011)	Spain	Multilayer Perceptron's	Latitude, longitude, day of the year, daily clear sky global radiation, cloud cover, total column ozone and water vapor	Predict solar radiation
Khatib et al (2012)	Malaysia	Multilayer Perceptron's	Latitude, longitude, days number and sunshine ratio	Solar irradiation
Khatib et al (2011)	Malaysia	Linear, nonlinear, fuzzy logic and ANN models	Latitude, longitude, day number and sunshine ratio	Global solar energy
Elminir et al (2005)	Aswan	Multilayer Perceptron's	Wind direction, wind velocity, ambient temperature, relative humidity, cloudiness and water vapor	Global insolation
Khatib et al (2012)	Malaysia	Multilayer Perceptron's	Latitude, longitude, days number and sunshine ratio	Solar irradiation
Khatib et al (2011)	Malaysia	Linear, nonlinear, fuzzy logic and ANN models	Latitude, longitude, day number and sunshine ratio	Global solar energy
Elminir et al (2005)	Aswan	Multilayer Perceptron's	Wind direction, wind velocity, ambient temperature, relative humidity, cloudiness and water vapor	Global insolation
Tymvios et al (2005)	Cyprus	Artificial neural networks and Angström	Theoretical daily sunshine duration, measured daily, sunshine duration, month, daily maximum temperature, monthly mean value of theoretical sunshine duration, monthly mean value of measured sunshine duration	Solar radiation

Table 2.2 (Continued)

References	country	Model	Input	Output
Benghanem et al (2009)	Saudi Arabia	Artificial neural networks	Different combination of air temperature, relative humidity, sunshine duration and the day of year	Daily global solar radiation
Fadare (2009)	Nigeria	Artificial neural networks	Latitude, longitude, altitude, month, mean sunshine duration, mean temperature, and relative humidity	Global solar radiation
Azadeh et al (2009)	Iran	Integrated ANN-Multilayer Perceptron's	Location, month, mean value of maximum temperature, minimum temperature, relative humidity, vapor pressure, total precipitation, wind speed and sunshine hour	Global solar radiation
Rahimikhoob (2010)	Iran	Artificial neural networks	Maximum and minimum air temperature, extraterrestrial radiation	Global solar radiation
Hasni et al (2012)	Algeria	Artificial neural networks	Air temperature, relative humidity	Global solar radiation
Koca et al (2011)	Turkey	Multilayer Perceptron's	Latitude, longitude, altitude, months, average temperature, average cloudiness, average wind velocity and sunshine duration	Global solar radiation
Mubiru et al (2008)	Uganda	Feed forward backpropagation Artificial neural networks; Levenberg–Marquard	Annual average of sunshine hours, cloud cover, relative humidity, rainfall, latitude, longitude and altitude	Global solar irradiation

CHAPTER III

Methodology

Material and methods

The research design, participants/sample, data collecting and analysis processes, as well as how the findings are analyzed, are all covered in this chapter. (The components in this section might be sorted based on the research's field of study and methodology.)

Study area

Jordan (Figure 3.1) is situated in the centre of the Middle East region, with a total size of 89,342km2. Jordan has a climate that is a mix of Mediterranean and semi-arid. Furthermore, annual precipitation varies from less than 50 millimetres in the eastern and southern deserts to 600 millimetres in the northern highlands. Jordan's weather is warm and dry in the summer and pleasant and humid in the winter. In the desert regions, average yearly temperatures vary from 12 to 25 degrees Celsius, with maximum temperatures reaching 35 degrees Celsius in the summer. Winter is the only time when it rains. Furthermore, there are roughly 310 bright days each year on average. The average annual worldwide horizontal and direct normal sun radiation in Amman, according to the Global Solar Atlas, is projected to be 5.850kWh/m2/day and 6.862kWh/m2/day, respectively.

In addition, the annual specific PV power output in Amman is 1877.8 kWh/kWp. According to the Global Wind Atlas, the mean wind power density is 58 W/m2 and 133 W/m2, respectively, which are rated as low by wind power density categorization at 10m/s and 50m/s. Finally, it is established that, in comparison to the wind speed, Amman has a large solar potential.

A PV system with a capacity of 68kW was developed, built, and tested in this study. This project's experimental work will be carried out in a specific building in Amman, Jordan, which is located at 31.953296°N, 35.907528°E and is approximately 950 feet above sea level.

Figure 3.1

Map of Jordan

Meteorological parameters measurement

Wet-bulb temperature, relative humidity, global solar radiation, and wind speed were a few of the daily measurements captured by the weather monitoring system. For this study, daily weather data were collected between January 1, 2020, and December 31, 2020.

PV system

As illustrated in Figure 3.2, the grid-connected PV system employed in this study is positioned on a flat building component. There are 183 modules in the PV system, with peak outputs ranging from 350 to 370 watts (All of these modules are Mono Crystalline Jinkosolar).

With a total surface of 1098 m2, the system has a total installed capacity of 68 kW. Inside the system, there are three PV-inverters of varied sizes pointed southerly at a fixed angle of 5.5 degrees, Azimuth angle 27. (15kW and 25kW). This system, on the other hand, was designed primarily to function as a power supply. During the monitoring period, Monitoring was performed of in-panel irradiation totals, array output power, and system energy output power. Based on the performance statistics collected at one-hour intervals, the built-in web server on the inverter computed hourly, weekly, and monthly performance statistics Tables 3.1 and 3.2 list the specification of selected PV panels and inverter, respectively.

Figure 3.2

Photo of PV System Located in The Selected Building in Amman, Jordan

Table 3.1

Specification of The PV Panel Used (Module type: JKM370M-72-V)

Variables	**Standard Test Conditions**	**Nominal Operating Cell Temperature**
Maximum Power (Pmax)	370Wp	278Wp
Maximum Power Voltage (Vmp)	39.9 V	38.1 V
Maximum Power Current (Imp)	9.28 A	7.30 A
Open-circuit Voltage (Voc)	48.5 V	47.0 V
Short-circuit Current (Isc)	9.61 A	7.75 A
Module Efficiency STC (%)	18.01%	
Operating Temperature(℃)	(-40℃~+85℃)	
Maximum system voltage	1500 VDC (IEC)	
Maximum series fuse rating	20 A	
Power tolerance	0~+3%	
Temperature coefficients of Pmax	(-0.40%/℃)	
Temperature coefficients of Voc	(-0.29%/℃)	
Temperature coefficients of Isc	(0.048%/℃)	
Nominal operating cell temperature (NOCT)	45±2℃	

Table 3.2

Specification of the inverters used

Input data	**ECO 25-3-S**	**ECO 20-3-S**
Max.input current	44.2A	33.0 A / 27.0 A
Max array short circit current	71.6 A	49.5 A / 40.5 A
DC input voltage range	580-1000 V	200 - 1000 V
Usable MPP Voltage range	650 V	200 V
Feed in start voltage	580-850 V	200 - 800 V
Number of DC connections	6	3+3
Max PV generator output	37.8KW peek	30.0 kWpeak
Output data	**ECO 25-3-S**	**ECO 20-3-S**
Max output power	25,000 VA	20,000 VA
AC output current	37.9 A / 36.2 A	28.9 A
Grid Connection (Voltage Range)	3~NPE 380 V / 220 V or 3~NPE 400 V / 230 V (+20 % / - 30 %)	3-NPE 400 V / 230 V or 3~NPE 380 V / 220 V (+20 % / -30 %)
Frequency (frequency range)	50 Hz / 60 Hz (45 - 65 Hz)	50 Hz / 60 Hz (45 - 65 Hz)
Total harmonic distortion	< 2.0 %	1.30%
Power factor (cos φac,r)	0 - 1 ind. / cap.	0 - 1 ind. / cap.

Empirical models

Artificial neural networks (ANN)

Machine learning models have been used to characterize complex systems (Livingstone 2009; Keat et al., 2015; Kassem et al., 2019; Kassem et al. 2018; Gökçekuş et al. 2020). They are used in a wide range of engineering and research applications. Four empirical models are built in this study to forecast PV output: Multilayer feed-Forward Neural Network (FFNN), Cascade Forward Neural Network (CFNN), Radial Basis Function Neural Network (RBFNN), and Elman neural network (ENN). The explanatory input variables in this study include Day (D), relative humidity (RH), average temperature (AT), maximum temperature (Tmax), lowest temperature (Tmin), wet-bulb temperature (Tw), wind speed (WS), and global solar radiation (GSR). The data is separated into training and testing groups, and the models' output is compared to each other. In this study, data was used to teach participants for eight months. And the developed model was used to predict remaining months, and then compared with actual data. Table 3.3 lists the developed models with various input combinations as shown in Table

Multilayer feed-forward neural network (MFFNN)

Three layers make up the MFFNN (input layer, hidden layer, and output layer). The number of neurons and hidden layers should be carefully chosen since they have an impact on training accuracy. TRAINLM is used for training purposes. In addition, the Mean Squared Error (MSE) is calculated to determine the training algorithm's optimal performance. The back-propagation algorithm's decreasing gradient is used to lower the MSE between the actual and estimated output. Kassem and Gokcekus provided a description of the created model (2021). Figure 3.3 depicts the suggested MFFNN method's explaining process.

Cascade feed-forward neural network (CFNN)

CFNN stands for a static neural network in which the signals only go forward (Alkhasawneh and Tay 2018). It's comparable to a feed-forward neural network, except it has a link between the input and every previous layer and the layers of the next layer (Hedayat et al. 2009; Zheng et al. 2020).

This model has the benefit of displaying nonlinear relationships without removing the linear link between input and output. The minimal value of RMSE is used to determine the optimal number of neurons. Kassem and Gokcekus provided a description of the created model (2021). The suggested model's phases are depicted in Figure 3.4 (CFNN).

Radial basis neural networks (RBFNN)

A feed-forward network with one input layer, one hidden layer, and one output layer is known as an RBFNN. Radial basis functions are utilized as activation functions (Pham et al. 2018). Due to their basic structure, RBFNN models have the most significant benefits over other multi-layer perceptron models in terms of speed and efficiency. Kassem and Gokcekus provided a description of the created model (2021). The suggested model's phases are depicted in Figure 3.5 (RBFNN).

Elman neural network (ENN)

A simple form of recurrent neural network is the ENN. The input layer, context layer, hidden layer, and output layer are the four primary layers (Yu et al. 2019). The basic structure of the ENN is comparable to that of a multilayer neural network. As previously indicated, ENN has a context layer, whose inputs originate from the hidden layer's outputs, which were used to store the hidden layer's output values from the prior time (Yu et al. 2017; Liu et al. 2018).

Table 3.3

57 Models With Different Input Combinations

Model number	Inputs	Model number	Inputs
#1	D	#2	Ta
#3	Tmax	#4	Tmin
#5	Tw	#6	GSR
#7	WS	#8	RH
#9	Ta, Tmax	#10	Ta, Tmin
#11	Ta, Tw	#12	Ta, GSR
#13	Ta, WS	#14	Ta, RH
#15	Tmax, Tmin	#16	Tmax, Ta
#17	Tmax, Tw	#18	Tmax, WS
#19	Tmax, RH	#20	Tmin, Tw
#21	Tmin, GSR	#22	Tmin, WS
#23	Tmin, RH	#24	Tw, GSR
#25	Tw, WS	#26	Tw, RH
#27	GSR,WS	#28	GSR,RH
#29	WS, RH	#30	D, Ta
#31	D, Tmax	#32	D, Tmin
#33	D, Tw	#34	D,GSR
#35	D, Ws	#36	D,RH
#37	D, Ta, Tmax	#38	D, Ta, Tmin
#39	D, Ta, Tw	#40	D, Ta, GSR
#41	D, Ta, WS	#42	D, Ta, RH
#43	D, Ta, Tmax, Tmin	#44	D, Ta, Tmax, Tw
#45	D, Ta, Tmax, GSR	#46	D, Ta, Tmax, WS
#47	D, Ta, Tmax, RH	#48	D, Ta, Tmax, Tmin, Tw
#49	D, Ta, Tmax, Tmin, GSR	#50	D, Ta, Tmax, Tmin, WS
#51	D, Ta, Tmax, Tmin, RH	#52	D, Ta, Tmax, Tmin, Tw, GSR
#53	D, Ta, Tmax, Tmin, Tw, WS	#54	D, Ta, Tmax, Tmin, Tw, RH
#55	D, Ta, Tmax, Tmin, Tw, GSR, WS	#56	D, Ta, Tmax, Tmin, Tw, GSR, RH
#57	D, Ta, Tmax, Tmin, Tw, GSR, WS, RH		

Figure 3.3

The Proposed Algorithm of Predicting PV-Output Using MFFNN

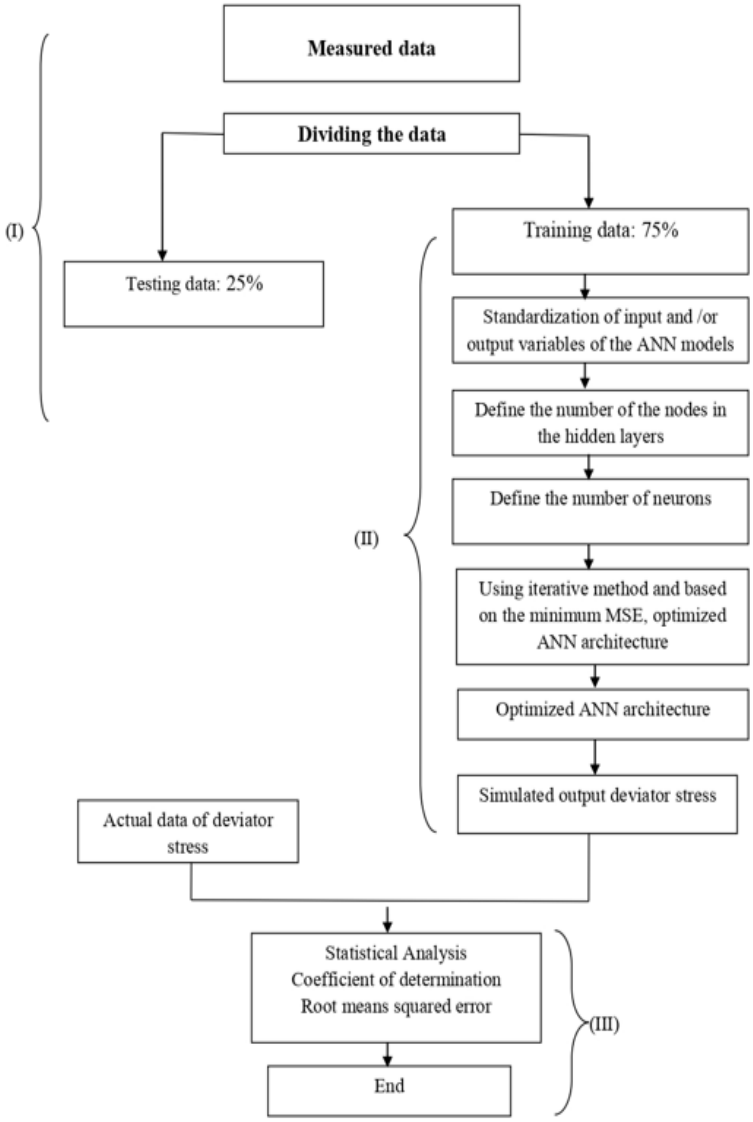

Figure 3.4

The proposed Algorithm of Predicting PV-Output Using CFNN

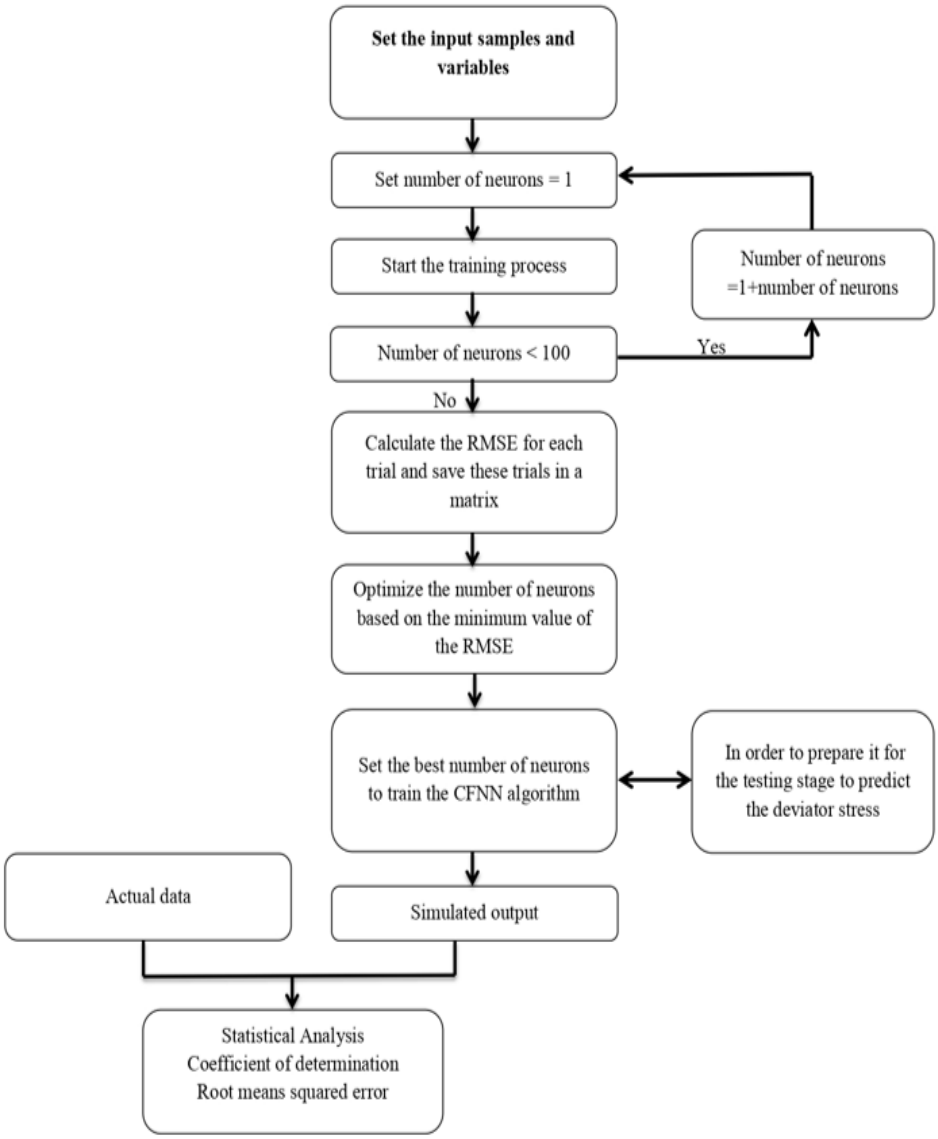

Figure 3.5

The Proposed Algorithm of Predicting PV-Output Using CFNN

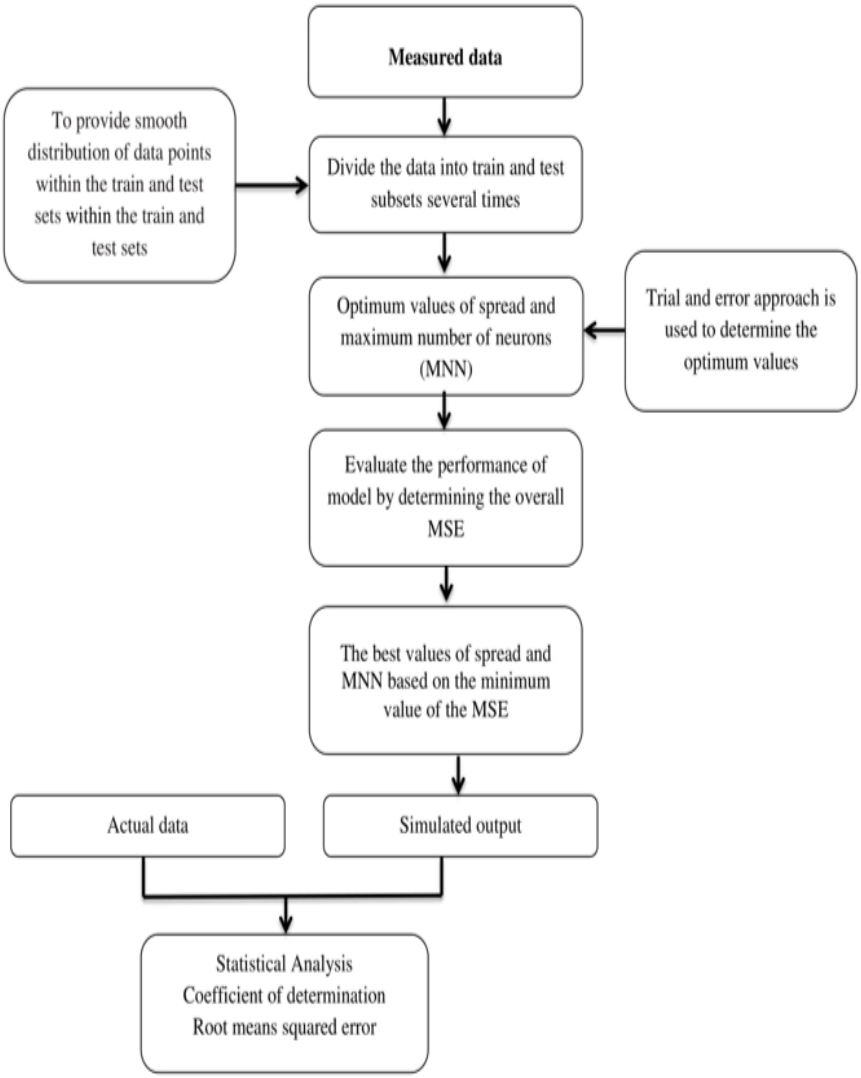

Quadratic model (QM)

The QM is a mathematical model that can represent both input and output variables that are influenced by input factors. The goal of this model is to determine the degree of effect of the input variables (Day (D), relative humidity (RH), average temperature (AT), maximum temperature (Tmax), minimum temperature (Tmin), wet temperature (Tw), wind speed (WS), and global solar radiation (GSR)) on the output parameter (PV-output) of a 68kW grid-connected PV system. The connection form between the input and output parameters is shown in Eq. (1).

$$PV - output = f(D, RH, Ta, Tmax, Tmin, Tw, WS, GSR) \quad (01)$$

Based on the actual data, regression analysis was carried out by the following quadratic polynomial model:

$$Y = \beta_0 + \sum_{i=1}^{n} \beta_i x_i + \sum_{i=1}^{n} \beta_{ii} x_i^2 + \sum_{i}^{n-1} \sum_{i=i+1}^{n} \beta_{ij} x_i x_j \quad (02)$$

Where Y is the predicted response, β_0 a constant, β_i the linear coefficient, β_{ii} the squared coefficient, and β_{ij} the cross-product coefficient, n is the number of factors, x_i and x_j are the independent variables.

Multiple linear regressions (MLR)

MLR is a classical method, which attempts to model the correlation between independent variables (x) and dependent (y). It explores how the dependent and independent variables are correlated. The MLR model is

$$Y = \beta_0 + \beta_1 x_1 + \cdots + \beta_i x_i \quad i = 1,2 \ldots n \quad (03)$$

Where Y is the predicted response, β_0 a constant, β_i the intercept and x_i where *i=1, 2,..,n*, denotes the explanatory or independent variables

Model performance criteria

The performance of the proposed models were evaluated based on the following equations:

R-squared

$$R^2 = 1 - \frac{\sum_{i=1}^{n}\left(a_{a,i} - a_{p,i}\right)^2}{\sum_{i=1}^{n}\left(a_{p,i} - a_{a,ave}\right)^2} \quad (04)$$

Mean squared error

$$MSE = \frac{1}{n}\sum_{i=1}^{n}\left(a_{a,i} - a_{p,i}\right)^2 \quad (05)$$

Root mean squared error

$$RMSE = \sqrt{\frac{1}{n}\sum_{i=1}^{n}\left(a_{a,i} - a_{p,i}\right)^2} \quad (06)$$

Mean absolute error

$$MAE = \frac{1}{n}\sum_{i=1}^{n}\left|a_{a,i} - a_{p,i}\right| \quad (07)$$

CHAPTER IV

Result and Discussions

Characteristics of measuring data

Table 4.1 shows the summary statistics for the machine learning models' input and output variables (day (D), relative humidity (RH), average temperature (AT), maximum temperature (Tmax), lowest temperature (Tmin), wet temperature (Tw), wind speed (WS), and global solar radiation (GSR). Furthermore, Figure 4.1 depicts the daily fluctuation of the study's assessed variables. The greatest PV output of 451.25 MWh was recorded in May, while the lowest figure of 32.83 MWh was recorded in January. Furthermore, as indicated in Figure 4.1, the highest temperature of 46.03°C is recorded in September, while the lowest temperature of 0.92 is recorded in February. Wind speed measurements range from 1.12 m/s in March to 7.31 m/s in February, according to the data.

Table 4.1

Statistical Parameters of Used Variables

Variable	Unit	Mean	SD	CV	Minimum	Maximum
D	-	183.5	105.8	57.66	1	366
RH	%	54.027	15.285	28.29	17.77	88.16
Ta	℃	21.308	7.394	34.7	5.49	36.41
Tmin	℃	15.441	6.298	40.79	0.92	28.98
Tmax	℃	28.799	8.927	31	10.65	46.03
Tw	℃	10.599	4.137	39.03	-0.54	19.58
WS	m/s	3.2697	1.1058	33.82	1.12	7.31
GSR	W/m^2	4925.1	1701.5	34.55	521	8377
PV-output	MWh	272.94	99.2	36.34	32.83	451.25

Figure 4.1

Daily Variation of Measurement Data During the Investigation Period.

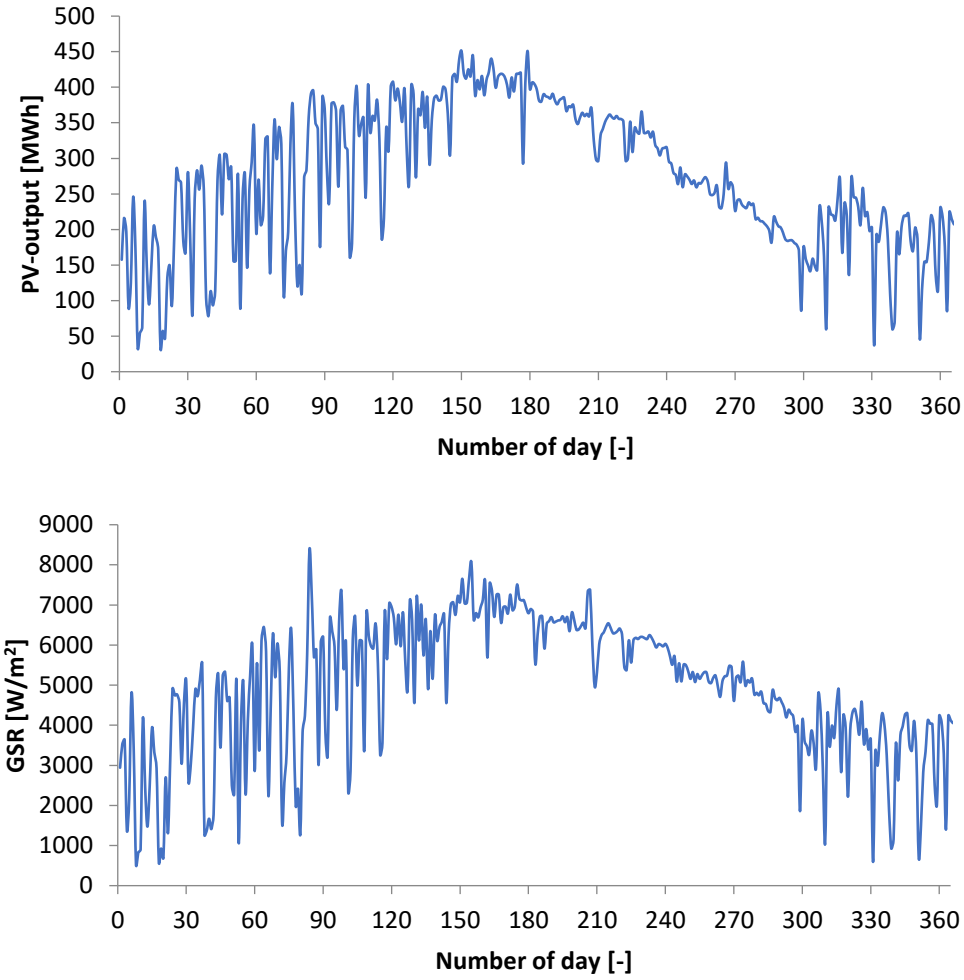

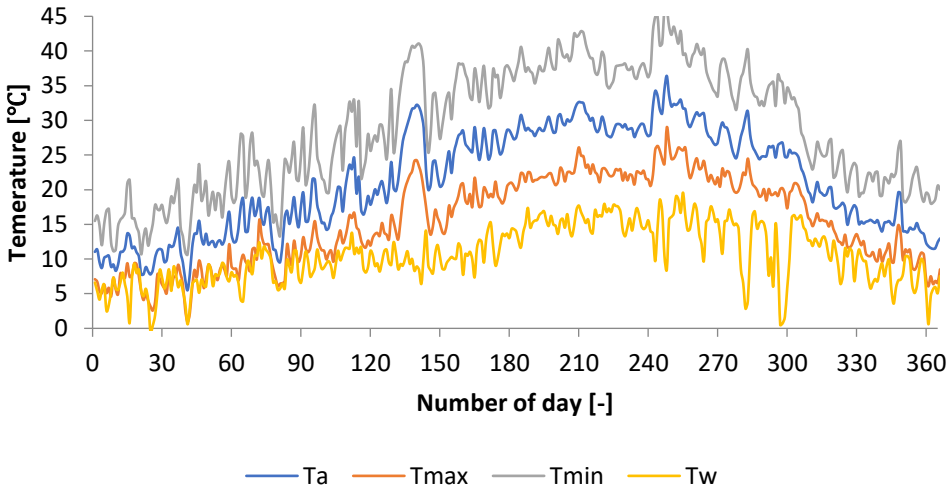

Figure 4.1 (Continued)

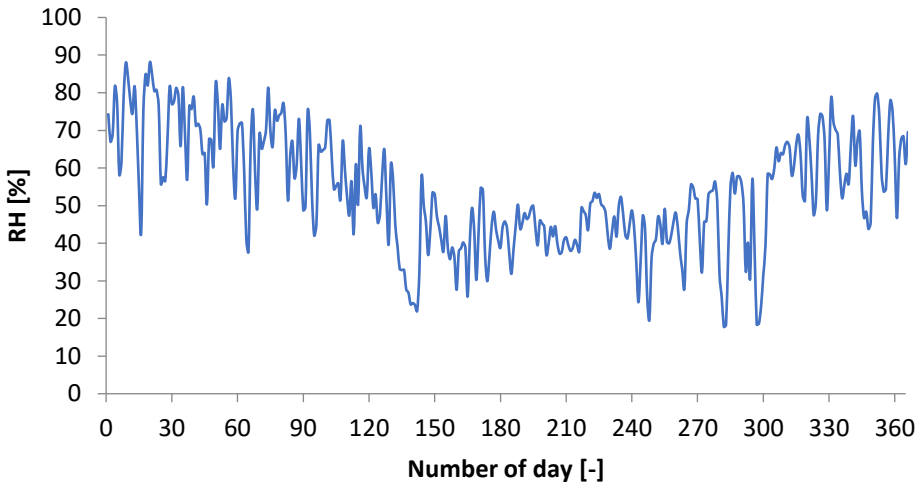

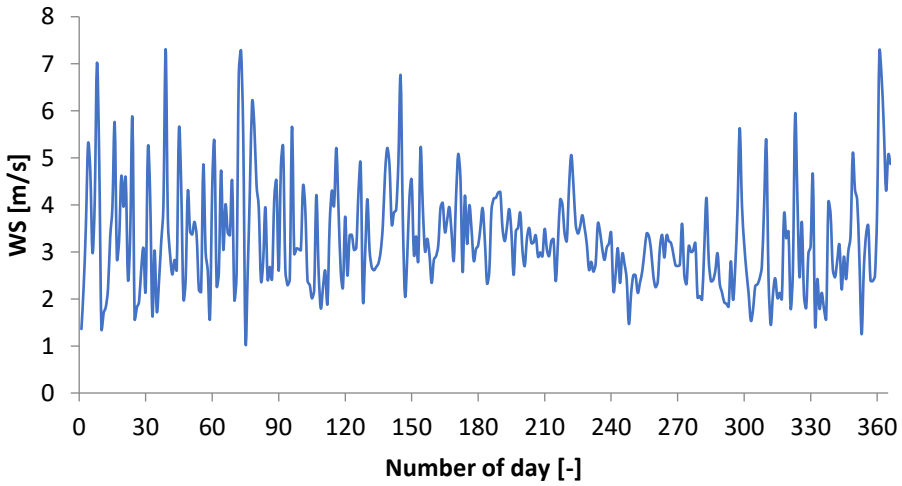

Machine learning models

Evaluate the influence of input variables

Three neural network models were used to forecast the PV output of a solar system in Amman, Jordan, as previously indicated. As a result, explanatory input variables include Day (D), relative humidity (RH), average temperature (AT), maximum temperature (Tmax), lowest temperature (Tmin), wet temperature (Tw), wind speed (WS), and global solar radiation (GSR). The data was split into training and testing groups, and the models' outcomes were compared against each other. In this study, data for 10 months was used to train the model, which was then used to forecast the remaining months and compared to the actual data. 57 models with varied input combinations were constructed in this study. to find the most influencing input parameters for estimating the output power of PV system. As mentioned previously, the optimum number of hidden layer (HL), neurons number (NN) and transfer function (TF) were selected based on the minimum value of MSE.

Case 1: parameter selection for one input

Table 4.2 as supplemental material shows the best HL, NN, and TF for 8 models (Model#1-Model#8), which were chosen based on the lowest MSE value. For estimating the input, it was discovered that RBFNN performed the best, followed by ENN, FFNN, and CFNN. Furthermore, it was discovered that RBFNN#6 had the greatest R2 value of 0.8472, followed by ENN#6 with a value of 0.4565. Furthermore, ENN#2 has the lowest RMSE value of 0.0021, followed by MFFNN#7, which has the highest RMSE value of 0.0024

Case 2: parameter selection for two inputs

To test the accuracy of employing the discovered parameters, 28 models with varying two inputs were presented in this scenario. The acquired values of the statistical parameters for both the training (HL, NN, TF, and MSE) and testing phases were presented in Table 4.3 as supplemental material (R2 and RMSE). With R2 values of 0.9090 and 0.0007, respectively, ENN#24 with a combination of [Tw, GSR] has the greatest value of R2 and the lowest value of RMSE

Case 3: parameter selection for three inputs

Three parameters are used as input variables for the suggested models in this scenario. As a result, five models with varied combinations were created, as presented in Table 4.4 as supplementary material. RBFNN#40, when used in conjunction with [D,Ta,GSR], yielded the greatest R2 value of 0.7420. Furthermore, the combination of [D,Ta,Tw] results in a minimal RMSE of 0.0023 for MFFNN#39.

Case 4: parameter selection for four inputs

As indicated in Table 4.5 as supplemental material, five models were created with distinct four different input factors in this example to find the most input variables that impact the estimation of power output of the PV system. RBFNN#45 [D,Ta,Tmax,GSR] is shown to be the best combination for calculating the power output of the PV system, followed by ENN#46 [D,Ta,Tmax,WS] based on the value of R2. Furthermore, MFFNN#44 yielded the lowest RMSE value of 0.0026, according to the results.

Case 5: parameter selection for five inputs

The performance of the suggested models with five input variables is summarized in Table 4.6 as supplemental material. With R2 values of 0.5059 and 0.0082, respectively, the ENN#48 [D,Ta,Tmax,Tmin,Tw] and RBFNN#50 [D,Ta,Tmax,Tmin,WS] yielded the greatest R2 value and the lowest RSME.

Case 6: parameter selection for six inputs

To estimate the PV system's power production, three models with six input variables were presented. As demonstrated in Table 4.7 as supplemental material, the highest R2 value and minimum RMSE value for MFFNN#52 are recorded using a combination of [D,Ta,Tmax,Tmin,Tw,GSR].

Case 7: parameter selection for seven inputs

Seven parameters are included as input variables for the suggested models in this example. As demonstrated in Table 4.8 as supplemental material, ENN#56 yielded the highest R2 and lowest RMSE with values of 0.8168 and 0.0011, respectively.

Case 8: parameter selection for eight inputs

All input variables are used as input parameters for the suggested models in this scenario. As shown in Table 4.9 as supplemental material, CFNN#57 with a combination of [D, Ta, Tmax, Tmin, Tw, GSR, WS, RH] has demonstrated high prediction accuracy with values of R2 and RMSE of 0.8623 and 0.0011, respectively.

Comparative analysis

The model ranking is investigated in this part based on the RMSE value, as shown in Tables 4.10 - 4.13 for machine learning models. The best models for predicting the PV-output of a 68kW grid-connected PV system are MFFNN#19, CFNN#12, ENN#24, and RBFNN#32, which use a mixture of [Tmax, RH], [Ta, GSR], [Tw, GSR], and [D, Tmin], respectively. The ENN#24 model has the lowest RMSE among the MFFNN#19, CFNN#12, ENN#24, and RBFNN#32 models, with a value of 0.00070. The most important characteristics that determine the performance of a PV system, according to the literature, are air temperature, relative humidity, and global solar radiation. Furthermore, the ambient temperature has a significant impact on global sun radiation forecasts.

For example, Meenal and Selvakumar (2018), Yadav et al. (2014), and Rao et al. (2018) discovered that ambient temperature, relative humidity, and sunlight hours were the most critical factors affecting solar radiation availability. Yesilata and Firatoglu (2008) determined that global solar radiation has an impact on the solar system's power production. Furthermore, the data suggest that the temperature of the wet bulb had a major effect in forecasting PV production. This was confirmed by several scientific researchers (Hosseini et al. 2019; Simsek et al. 2021). Hosseini et al. (2019) looked into the effect of dew formation on solar panel performance.

The results indicated that as the quantity of dew on the module's surface rose, the performance of the solar panel reduced. Simsek et al. (2021) investigated the impact of dew development on PV panel performance. They discovered that when the amount of dew formation increased, the energy generation of PV panels reduced dramatically. Finally, it can be argued that two parameter combinations of input variables are sufficient for accurately estimating the PV-output.

Table 4.10

Ranking of MFFNN Models Based on RMSE

Model	Input variables								RMSE	Rank
	D	Ta	Tmax	Tmin	Tw	GSR	WS	RH		
MFFNN#19			+					+	0.00224	1
MFFNN#39	+	+			+				0.00230	2
MFFNN#7							+		0.00235	3
MFFNN#52	+	+	+	+	+	+			0.00247	4
MFFNN#44	+	+	+		+				0.00258	5
MFFNN#21				+		+			0.00303	6
MFFNN#40	+	+				+			0.00356	7
MFFNN#53	+	+	+	+	+		+		0.00359	8
MFFNN#42	+	+						+	0.00362	9
MFFNN#14		+						+	0.00396	10
MFFNN#35	+						+		0.00406	11
MFFNN#41	+	+					+		0.00418	12
MFFNN#29							+	+	0.00441	13
MFFNN#16			+		+				0.00479	14
MFFNN#47	+	+	+					+	0.00516	15
MFFNN#37	+	+	+						0.00539	16
MFFNN#26					+			+	0.00637	17
MFFNN#15			+	+					0.00640	18
MFFNN#8								+	0.00642	19
MFFNN#36	+							+	0.00642	20
MFFNN#30	+	+							0.00650	21
MFFNN#32	+			+					0.00668	22
MFFNN#4				+					0.00675	23
MFFNN#9		+	+						0.00699	24
MFFNN#20				+	+				0.00740	25
MFFNN#2		+							0.00887	26
MFFNN#56	+	+	+	+	+	+		+	0.01031	27
MFFNN#49	+	+	+	+		+			0.01064	28
MFFNN#5					+				0.01141	29
MFFNN#3			+						0.01500	30
MFFNN#11		+			+				0.01658	31
MFFNN#50	+	+	+	+			+		0.01660	32
MFFNN#22				+			+		0.01704	33
MFFNN#10		+		+					0.01788	34
MFFNN#28						+		+	0.02624	35
MFFNN#43	+	+	+	+					0.03273	36
MFFNN#17			+			+			0.03335	37
MFFNN#18			+				+		0.04094	38
MFFNN#55	+	+	+	+	+	+	+		0.04477	39
MFFNN#34	+					+			0.05396	40
MFFNN#31	+		+						0.06436	41
MFFNN#23				+				+	0.07303	42
MFFNN#12		+				+			0.07509	43
MFFNN#27						+	+		0.08117	44
MFFNN#13		+					+		0.08670	45
MFFNN#51	+	+	+	+				+	0.10213	46
MFFNN#33	+				+				0.10297	47
MFFNN#24					+	+			0.10367	48

Table 4.10 (Continued)

Model	Input variables								RMSE	Rank
	D	Ta	Tmax	Tmin	Tw	GSR	WS	RH		
MFFNN#38	+	+		+					0.10406	49
MFFNN#48	+	+	+	+	+				0.11440	51
MFFNN#57	+	+	+	+	+	+	+	+	0.11602	52
MFFNN#1	+								0.11967	53
MFFNN#6						+			0.12077	54
MFFNN#46	+	+	+				+		0.14762	55
MFFNN#54	+	+	+	+	+			+	0.15865	56
MFFNN#45	+	+	+			+			0.18034	57

Table 4.11

Ranking of CFNN Models Based on RMSE

Model	Input variables								RMSE	Rank
	D	Ta	Tmax	Tmin	Tw	GSR	WS	RH		
CFNN#12		+				+			0.000997	1
CFNN#57	+	+	+	+	+	+	+	+	0.001087	2
CFNN#14		+						+	0.001638	3
CFNN#37	+	+	+						0.001645	4
CFNN#54	+	+	+	+	+			+	0.004195	5
CFNN#31	+		+						0.004562	6
CFNN#36	+							+	0.005446	7
CFNN#21				+		+			0.005655	8
CFNN#25					+		+		0.006613	9
CFNN#24					+	+			0.006681	10
CFNN#40	+	+				+			0.006941	11
CFNN#35	+						+		0.006992	12
CFNN#18			+				+		0.008743	13
CFNN#34	+					+			0.009424	14
CFNN#22				+			+		0.009561	15
CFNN#27						+	+		0.009791	16
CFNN#7							+		0.009883	17
CFNN#47	+	+	+					+	0.010575	18
CFNN#29							+	+	0.010643	19
CFNN#5					+				0.011171	20
CFNN#8								+	0.011396	21
CFNN#26					+			+	0.011588	22
CFNN#3			+						0.012888	23
CFNN#46	+	+	+				+		0.013639	24
CFNN#16			+		+				0.01399	25
CFNN#11		+			+				0.020908	26
CFNN#30	+	+							0.023197	27
CFNN#52	+	+	+	+	+	+			0.024015	28
CFNN#4				+					0.025058	29
CFNN#15			+	+					0.02579	30
CFNN#19			+					+	0.028703	31
CFNN#49	+	+	+	+		+			0.028775	32

Table 4.11 (Continued)

Model	Input variables								RMSE	Rank
	D	Ta	Tmax	Tmin	Tw	GSR	WS	RH		
CFNN#50	+	+	+	+			+		0.035575	33
CFNN#55	+	+	+	+	+	+	+		0.042679	34
CFNN#44	+	+	+		+				0.063617	35
CFNN#1	+								0.075403	36
CFNN#6						+			0.076376	37
CFNN#45	+	+	+			+			0.079251	38
CFNN#51	+	+	+	+				+	0.09061	39
CFNN#56	+	+	+	+	+	+		+	0.103742	40
CFNN#41	+	+					+		0.104388	41
CFNN#38	+	+		+					0.105749	42
CFNN#13		+					+		0.116951	43
CFNN#43	+	+	+	+					0.122549	44
CFNN#39	+	+			+				0.138521	45
CFNN#20				+	+				0.141946	46
CFNN#9		+	+						0.143538	47
CFNN#28						+		+	0.146937	48
CFNN#33	+				+				0.147018	49
CFNN#10		+		+					0.152145	50
CFNN#17			+			+			0.168132	51
CFNN#32	+			+					0.177411	52
CFNN#42	+	+						+	0.179998	53
CFNN#48	+	+	+	+	+				0.181134	54
CFNN#23				+				+	0.201018	55
CFNN#53	+	+	+	+	+		+		0.215223	56
CFNN#2		+							0.251434	57

Table 4.12

Ranking of ENN models based on RMSE

Model	Input variables								RMSE	Rank
	D	Ta	Tmax	Tmin	Tw	GSR	WS	RH		
ENN#24					+	+			0.00070	1
ENN#56	+	+	+	+	+	+		+	0.00106	2
ENN#31	+		+						0.00167	3
ENN#2		+							0.00208	4
ENN#33	+				+				0.00234	5
ENN#26					+			+	0.00271	6
ENN#37	+	+	+						0.00282	7
ENN#17			+			+			0.00287	8
ENN#5					+				0.00292	9
ENN#38	+	+		+					0.00307	10
ENN#3			+						0.00316	11
ENN#20				+	+				0.00327	12
ENN#46	+	+	+				+		0.00351	13
ENN#7							+		0.00361	14

Table 4.12 (Continued)

Model	Input variables								RMSE	Rank
	D	Ta	Tmax	Tmin	Tw	GSR	WS	RH		
ENN#34	+					+			0.00426	15
ENN#16			+		+				0.00491	16
ENN#9		+	+						0.00494	17
ENN#29							+	+	0.00500	18
ENN#27						+	+		0.00510	19
ENN#14		+						+	0.00514	20
ENN#47	+	+	+					+	0.00516	21
ENN#19			+					+	0.00559	22
ENN#21				+		+			0.00578	23
ENN#30	+	+							0.00650	24
ENN#32	+			+					0.00668	25
ENN#40	+	+				+			0.00699	26
ENN#15			+	+					0.00699	27
ENN#10		+		+					0.00699	28
ENN#44	+	+	+		+				0.00699	29
ENN#11		+			+				0.00699	30
ENN#4				+					0.00699	31
ENN#28						+		+	0.00720	32
ENN#39	+	+			+				0.00982	33
ENN#49	+	+	+	+		+			0.01064	34
ENN#55	+	+	+	+	+	+	+		0.01478	35
ENN#23				+				+	0.01528	36
ENN#36	+							+	0.01998	37
ENN#48	+	+	+	+	+				0.02325	38
ENN#51	+	+	+	+				+	0.02533	39
ENN#53	+	+	+	+	+		+		0.02630	40
ENN#25					+		+		0.02798	41
ENN#42	+	+						+	0.04072	43
ENN#18			+				+		0.07213	44
ENN#43	+	+	+	+					0.10399	45
ENN#57	+	+	+	+	+	+	+	+	0.10859	46
ENN#1	+								0.11967	47
ENN#35	+						+		0.12023	48
ENN#6						+			0.12077	49
ENN#22				+			+		0.12879	50
ENN#50	+	+	+	+			+		0.12950	51
ENN#12		+				+			0.14100	52
ENN#8								+	0.14560	53
ENN#41	+	+					+		0.14748	54
ENN#45	+	+	+			+			0.18034	55
ENN#13		+					+		0.18081	56
ENN#54	+	+	+	+	+			+	0.22098	57

Table 4.13

Ranking of RBFNN models based on RMSE

Model	Inputs								RMSE	Rank
	D	Ta	Tmax	Tmin	Tw	GSR	WS	RH		
RBFNN#32	+			+					0.006636	1
RBFNN#5					+				0.006777	2
RBFNN#13		+					+		0.006910	3
RBFNN#38	+	+		+					0.006910	4
RBFNN#20				+	+				0.007014	5
RBFNN#21				+		+			0.007014	6
RBFNN#30	+	+							0.007193	7
RBFNN#7							+		0.007281	8
RBFNN#14		+						+	0.007402	9
RBFNN#22				+			+		0.007414	10
RBFNN#1	+								0.007443	11
RBFNN#18			+				+		0.007507	12
RBFNN#3			+						0.007526	13
RBFNN#9		+	+						0.007597	14
RBFNN#31	+		+						0.007917	15
RBFNN#19			+					+	0.008008	16
RBFNN#2		+							0.008010	17
RBFNN#4				+					0.008050	18
RBFNN#37	+	+	+						0.008148	19
RBFNN#46	+	+	+				+		0.008152	20
RBFNN#43	+	+	+	+					0.008167	21
RBFNN#41	+	+					+		0.008179	22
RBFNN#8								+	0.008213	23
RBFNN#25					+		+		0.008228	24
RBFNN#50	+	+	+	+			+		0.008232	25
RBFNN#29							+	+	0.008546	26
RBFNN#28						+		+	0.008668	27
RBFNN#17			+			+			0.008847	28
RBFNN#35	+						+		0.008904	29
RBFNN#45	+	+	+			+			0.009240	30
RBFNN#12		+				+			0.009247	31
RBFNN#34	+					+			0.009270	32
RBFNN#53	+	+	+	+	+		+		0.009286	33
RBFNN#40	+	+				+			0.009317	34
RBFNN#33	+				+				0.009554	35
RBFNN#47	+	+	+					+	0.009572	36
RBFNN#36	+							+	0.009575	37
RBFNN#42	+	+						+	0.009636	38
RBFNN#48	+	+	+	+	+				0.009756	39
RBFNN#11		+			+				0.009810	40

Table 4.13 (Continued)

Model	Input variables								RMSE	Rank
	D	Ta	Tmax	Tmin	Tw	GSR	WS	RH		
RBFNN#39	+	+			+				0.009819	41
RBFNN#52	+	+	+	+	+	+			0.009893	42
RBFNN#49	+	+	+	+		+			0.009957	43
RBFNN#56	+	+	+	+	+	+		+	0.010301	44
RBFNN#44	+	+	+		+				0.010473	45
RBFNN#16			+		+				0.010541	46
RBFNN#54	+	+	+	+	+			+	0.010620	47
RBFNN#24					+	+			0.011208	48
RBFNN#57	+	+	+	+	+	+	+	+	0.011322	49
RBFNN#26					+			+	0.011472	50
RBFNN#23				+				+	0.011968	51
RBFNN#10		+		+					0.012674	52
RBFNN#15			+	+					0.012705	53
RBFNN#27						+	+		0.013611	54
RBFNN#6						+			0.013630	55
RBFNN#55	+	+	+	+	+	+	+		0.014776	56
RBFNN#51	+	+	+	+				+	0.025326	57

Comparison of quadratic model (QM) and multiple linear regression (MLR) with machine learning models

To demonstrate the accuracy of the proposed model, the performance of machine learning models is compared to quadratic model (QM) and multiple linear regression (MLR) in this section. The models' estimating success was measured using root mean squared error (RMSE) and mean absolute error (MAR). The mathematical equations for the QM and MLR models, as well as the RMSE and MAE values for all models, are shown in Table 9. The ENN#24, ENN#56, CFNN#12, and CFNN#57, respectively, with the combination of [Tw, GSR], [D, Ta, Tmax, Tmin, Tw, GSR, RH], [Ta, GSR], and [D, Ta, Tmax, Tmin, Tw, GSR, WS, RH], have demonstrated the best prediction. The lowest error value was obtained by combining [Tw, GSR].

R-squared is a measure of how well a regression line fits the data in general, whereas RMSE and MAE are direct techniques for describing variances. For maximum precision, R-squared, the combination of [Tw, GSR] has the highest value of R-squared followed by [D, Ta, Tmax, Tmin, Tw, GSR, WS, RH], [Ta, GSR] and [D, Ta, Tmax, Tmin, Tw, GSR, RH] as shown in Figure 4.2

Table 4.14

Comparison of quadratic model (QM) and multiple linear regression (MLR) with machine learning models for testing data

QM and MLR with MFFNN			
Model	**Input**	**RMSE**	**MAE**
MFFNN#19	Tmax, RH	0.00224	0.00169
MLR		0.00677	0.00523
QM		0.00748	0.00647
MFFNN#39	D, Ta, Tw	0.00230	0.00161
MLR		0.00675	0.00544
QM		0.01021	0.00745
MFFNN#7	WS	0.00235	0.00190
MLR		0.00511	0.00439
QM		0.00551	0.00496
QM and MLR with MFFNN			
Model	**Input**	**RMSE**	**MAE**
CFNN#12	Ta, GSR	0.000997	0.000646
MLR		0.006993	0.005722
QM		0.007742	0.006076
CFNN#57	D, Ta, Tmax, Tmin, Tw, GSR, WS, RH	0.001087	0.000864
MLR		0.009543	0.007519
QM		0.014767	0.010652
CFNN#14	Ta, RH	0.001638	0.005722
MLR		0.007591	0.006915
QM		0.008219	0.001294
QM and MLR with MFFNN			
Model	**Input**	**RMSE**	**MAE**
ENN#24	Tw, GSR	0.0007	0.000512
MLR		0.008034	0.006541
QM		0.009321	0.006452
ENN#56	D, Ta, Tmax, Tmin, Tw, GSR, RH	0.001056	0.000617
MLR		0.009418	0.007652
QM		0.014344	0.010238
ENN#31	D, Tmax	0.00167	0.001397
MLR		0.006052	0.005642
QM		0.009118	0.006318
QM and MLR with MFFNN			
Model	**Input**	**RMSE**	**MAE**
RBFNN#32	D, Tmin	0.00664	0.00471
MLR		0.00510	0.00428
QM		0.00703	0.00536
RBFNN#5	Tw	0.00678	0.00591
MLR		0.00539	0.00415
QM		0.00537	0.00462
RBFNN#13	Ta, WS	0.00691	0.00638
MLR		0.00511	0.00448
QM		000685	0.00576

Comparison of quadratic model (QM) and multiple linear regression (MLR) with machine learning models for testing data:

QM and MLR with MFFNN

$$\mathrm{PV-output} = 0.0423 - 0.0219 \cdot \mathrm{T_{max}} - 0.0394 \cdot \mathrm{RH} \quad (08)$$

$$\mathrm{PV-output} = -0.134 + 0.314 \cdot \mathrm{Tmax} + 0.369 \cdot \mathrm{RH} - 0.168 \cdot (\mathrm{T})\mathrm{max}\,\hat{}\,2 - 0.243 \cdot (\mathrm{RH})\hat{}\,2 - 0.345 \cdot (\mathrm{T})\mathrm{max} \cdot \mathrm{RH} \quad (09)$$

$$\mathrm{PV-output} = -0.0184 - 0.0174 \cdot \mathrm{D} + 0.0263 \cdot \mathrm{T_a} - 0.0224 \cdot \mathrm{T_w} \quad (10)$$

$$\mathrm{PV-output} = 0.0067 - 0.126 \cdot \mathrm{D} + 0.251 \cdot \mathrm{T_a} - 0.0799 \cdot \mathrm{T_w} + 0.097 \cdot \mathrm{D^2} - 0.188 \cdot \mathrm{T_a^2} - 0.062\mathrm{T_w^2} - 0.109 \cdot \mathrm{D} \cdot \mathrm{T_a} + 0.0762 \cdot \mathrm{D} \cdot \mathrm{T_w} + 0.126 \cdot \mathrm{T_a} \cdot \mathrm{T_w} \quad (11)$$

$$\mathrm{PV-output} = 0.0145 - 0.0107 \cdot \mathrm{WS} \quad (12)$$

$$\mathrm{PV-output} = 0.0082 + 0.0257 \cdot \mathrm{WS} - 0.0417 \cdot (\mathrm{WS})\hat{}\,2 \quad (14)$$

QM and MLR with CFNN

$$\mathrm{PV-output} = -0.00354 - 0.00206 \cdot \mathrm{T_a} + 0.0443 \cdot \mathrm{GSR} \quad (15)$$

$$\mathrm{PV-output} = -0.0029 + 0.0221 \cdot \mathrm{T_a} + 0.0022 \cdot \mathrm{GSR} - 0.0433 \cdot \mathrm{T_a^2} + 0.0359 \cdot \mathrm{GSR^2} + 0.006 \cdot \mathrm{T_a} \cdot \mathrm{GSR} \quad (16)$$

$$\mathrm{V-output} = 0.0637 - 0.0115 \cdot \mathrm{D} - 0.066 \cdot \mathrm{RH} - 0.113 \cdot \mathrm{T_a} - 0.031 \cdot \mathrm{T_{min}} + 0.063 \cdot \mathrm{T_{max}} - 0.0396 \cdot \mathrm{T_w} - 0.0094 \cdot \mathrm{WS} + 0.0179 \cdot \mathrm{GSR} \quad (17)$$

$$\begin{aligned}\mathrm{PV-output} = {} & -1.08 - 0.056 \cdot \mathrm{D} + 2.19 \cdot \mathrm{RH} + 2.48 \cdot \mathrm{T_a} + 0.44 \cdot \mathrm{T_{min}} \\ & - 0.46 \cdot \mathrm{T_{max}} - 1.24 \cdot \mathrm{T_w} + 0.28 \cdot \mathrm{WS} + 0.698 \cdot \mathrm{GSR} + 0.193 \cdot \mathrm{D^2} \\ & - 1.01 \cdot \mathrm{RH^2} - 22.1 \cdot \mathrm{T_a^2} - 3.85 \cdot \mathrm{T_{min}^2} - 5.17 \cdot \mathrm{T_{max}^2} + 0.03 \cdot \mathrm{T_w^2} \\ & - 0.0573 \cdot \mathrm{WS^2} - 0.128 \cdot \mathrm{GSR^2} - 0.146 \cdot \mathrm{D} \cdot \mathrm{RH} + 0.23 \cdot \mathrm{D} \cdot \mathrm{T_a} \\ & - 0.249 \cdot \mathrm{D} \cdot \mathrm{T_{min}} - 0.236 \cdot \mathrm{D} \cdot \mathrm{T_{max}} + 0.156 \cdot \mathrm{D} \cdot \mathrm{T_w} - 0.0084 \cdot \mathrm{D} \\ & \cdot \mathrm{WS} - 0.118 \cdot \mathrm{D} \cdot \mathrm{GSR} - 2.6 \cdot \mathrm{RH} \cdot \mathrm{T_a} - 0.21 \cdot \mathrm{RH} \cdot \mathrm{T_{min}} + 1.00 \\ & \cdot \mathrm{RH} \cdot \mathrm{T_{max}} + 0.67 \cdot \mathrm{RH} \cdot \mathrm{T_w} - 0.272 \cdot \mathrm{RH} \cdot \mathrm{WS} - 0.71 \cdot \mathrm{RH} \cdot \mathrm{GSR} \\ & + 18.3 \cdot \mathrm{T_a} \cdot \mathrm{T_{min}} + 22.9 \cdot \mathrm{T_a} \cdot \mathrm{T_{max}} + 0.65 \cdot \mathrm{T_a} \cdot \mathrm{T_w} + 0.22 \cdot \mathrm{T_a} \\ & \cdot \mathrm{WS} - 0.60 \cdot \mathrm{T_a} \cdot \mathrm{GSR} - 11.18 \cdot \mathrm{T_{min}} \cdot \mathrm{T_{max}} + 0.67 \cdot \mathrm{T_{min}} \cdot \mathrm{T_w} \\ & - 0.13 \cdot \mathrm{T_{min}} \cdot \mathrm{WS} - 0.19 \cdot \mathrm{T_{min}} \cdot \mathrm{GSR} - 0.63 \cdot \mathrm{T_{max}} \cdot \mathrm{T_w} \\ & - 0.49 \cdot \mathrm{T_{max}} \cdot \mathrm{WS} + 0.12 \cdot \mathrm{T_{max}} \cdot \mathrm{GSR} + 0.225 \cdot \mathrm{T_w} \cdot \mathrm{WS} \\ & + 0.473 \cdot \mathrm{T_w} \cdot \mathrm{GSR} - 0.039 \cdot \mathrm{WS} \\ & \cdot \mathrm{GSR} \end{aligned} \quad (18)$$

$$\mathrm{PV-output} = 0.05 - 0.0307 \cdot \mathrm{T_a} - 0.0456 \cdot \mathrm{RH} \quad (19)$$

$$\begin{aligned}PV-output = {} & -0.061 + 0.208 \cdot T_a + 0.192 \cdot RH - 0.143 \cdot T_a^2 - 0.141 \cdot RH^2 \\ & - 0.197 \cdot T_a \cdot RH \end{aligned} \quad (20)$$

QM and MLR with ENN

$$\mathrm{PV-output} = 0.0026 - 0.0255 \cdot \mathrm{T_w} + 0.0398\mathrm{GSR} \quad (21)$$

$$\begin{aligned}&\mathrm{PV-output} \\ &= -0.014 + 0.0289 \cdot \mathrm{T_w} + 0.0371 \cdot \mathrm{GSR} + 0.0178 \cdot \mathrm{T_w^2} + 0.0678 \cdot \mathrm{GSR^2} \\ &+ 0.13 \cdot \mathrm{T_w} \cdot \mathrm{GSR} \end{aligned} \quad (22)$$

$$\begin{aligned}\mathrm{PV-output} = {} & 0.0526 - 0.0098 \cdot \mathrm{D} - 0.0577 \cdot \mathrm{RH} - 0.115 \cdot \mathrm{T_a} - 0.034 \cdot \mathrm{T_{min}} \\ & + 0.075 \cdot \mathrm{T_{max}} - 0.0355 \cdot \mathrm{T_w} + 0.0195 \cdot \mathrm{GSR} \end{aligned} \quad (23)$$

$$PV-output = -57 - 0.153 \cdot D + 1.00 \cdot RH + 2.22 \cdot T_a + 0.14 \cdot T_{min} - 4.25 \cdot T_{max} - 0.31 \cdot T_w + 0.466 \cdot GSR + 0.170 \cdot D^2 - 0.30 \cdot RH^2 - 23.1 \cdot T_a^2 - 3.95 \cdot T_{min}^2 - 5.67 \cdot T_{max}^2 + 0.36 \cdot T_w^2 - 0.103 \cdot GSR^2 + 0.008 \cdot D \cdot RH + 0.24 \cdot D \cdot T_a - 0.210 \cdot D \cdot T_{min} - 0.073 \cdot D \cdot T_{max} + 0.025 \cdot D \cdot T_w - 0.102 \cdot D \cdot GSR - 1.83 \cdot RH \cdot T_a + 1.59 \cdot RH \cdot T_{max} - 0.41 \cdot RH \cdot T_w - 0.439 \cdot RH \cdot GSR + 19.1 \cdot T_a \cdot T_{min} + 24.9 \cdot T_a \cdot T_{max} + 0.07 \cdot T_a \cdot T_w - 0.76 \cdot T_a \cdot GSR - 11.60 \cdot T_{min} \cdot T_{max} + 059 \cdot T_{min} \cdot T_w - 0.10 \cdot T_{min} \cdot GSR - 1.02 \cdot T_{max} \cdot T_w + 0.48 \cdot T_{max} \cdot GSR + 0.262 \cdot T_w \cdot GSR \quad (24)$$

$$\mathrm{PV-output} = 0.01225 - 0.0195 \cdot \mathrm{D} + 0.0161 \cdot \mathrm{T_{max}} \quad (25)$$

$$\mathrm{PV-output} = -0.0052 - 0.132 \cdot \mathrm{D} + 0.1765 \cdot \mathrm{T_{max}} + 0.1337 \cdot \mathrm{D^2} - 0.0655 \cdot \mathrm{T_{max}^2} + 0.1114 \cdot \mathrm{D} \cdot \mathrm{T_{max}} \quad (26)$$

QM and MLR with RBFNN

$$PV-output = 0.01521 - 0.017 \cdot D + 0.0078 \cdot T_{min} \quad (27)$$

$$PV-output = -0.0112 - 0.019 \cdot D + 0.139 \cdot T_{min} + 0.0163 \cdot D^2 - 0.0937 \cdot T_{min}^2 - 0.0552 \cdot D \cdot T_{min} \quad (28)$$

$$\mathrm{PV-output} = 0.01595 - 0.0094 \cdot \mathrm{T_w} \quad (29)$$

$$\mathrm{PV-output} = 0.0041 + 0.0413 \cdot \mathrm{T_w} - 0.0464 \cdot \mathrm{T_w^2} \quad (30)$$

$$\mathrm{PV-output} = 0.0129 + 0.0028 \cdot \mathrm{T_a} - 0.0102 \cdot \mathrm{WS} \quad (31)$$

$$\mathrm{PV-output} = -0145 + 0.0961 \cdot \mathrm{T_a} + 0.0475 \cdot \mathrm{WS} - 0.0815 \cdot \mathrm{T_a^2} + 0.0472 \cdot \mathrm{WS^2} - 0.0417 \cdot \mathrm{T_a} \cdot \mathrm{WS} \quad (32)$$

Figure 4.2

Comparison between actual and forecasted values by all the best combination of inputs

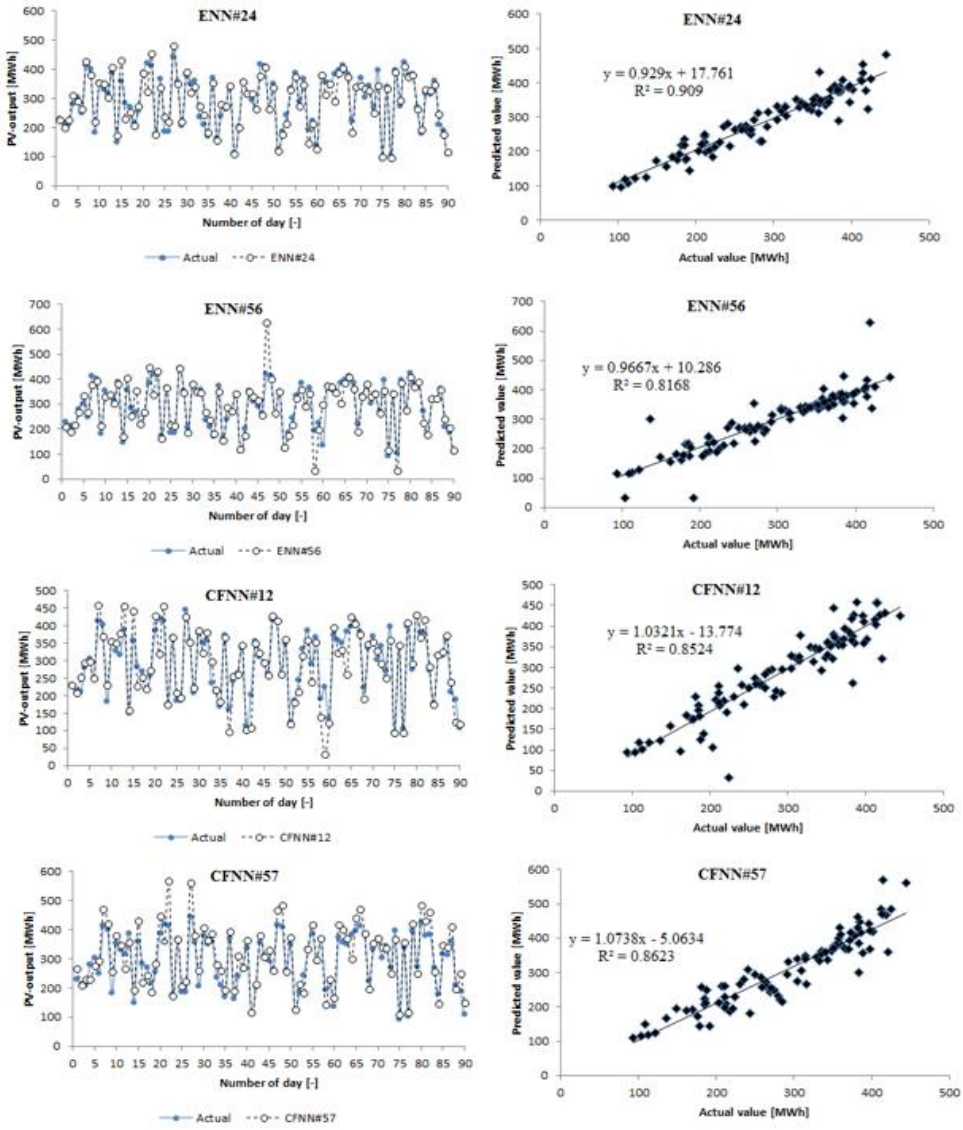

CHAPTER V

Conclusion and Recommendations

Conclusions

The influence of meteorological conditions on PV system output power (PV-output) was explored in this study. By varying the weather parameters, six models were developed to address the main objective: quadratic model (QM), multiple linear regression (MLR), aMultilayer Feed-Forward Neural Network (MFFNN), Cascade Feed-Forward Neural Network (CFNN), Radial Basis Neural Network (RBFNN), and Elman neural network (ENN).

The models were developed using a one-year database of daily relative humidity (RH), average temperature (AT), maximum temperature (Tmax), minimum temperature (Tmin), wet-bulb temperature (Tw), wind speed (WS), and global solar radiation (GSR), as well as measuring the value of PV system output power (PV-output). To train and test the models, 57 models with various combinations of inputs are used to train and test them in order to find the optimal combination of inputs for estimating daily PV output.

The ENN#24, ENN#56, CFNN#12, and CFNN#57 with the combination of [Tw, GSR], [D, Ta, Tmax, Tmin, Tw, GSR, RH], [Ta, GSR], and [D, Ta, Tmax, Tmin, Tw, GSR, WS, RH], respectively, have shown the best prediction out of the 57 machine learning models.

Wet-bulb temperature, global solar radiation, and average temperature are shown to be the most important input parameters for projecting PV production. Furthermore, the findings showed that the ENN and CFNN models could be utilized to properly estimate the daily PV production for the site.

References

Aagreh, Y., & Al-Ghzawi, A. (2013). Feasibility of utilizing renewable energy systems for a small hotel in Ajloun city, Jordan. *Applied Energy*, 103, 25-31.https://doi.org/10.1016/j.apenergy.2012.10.008

Abujubbeh, M., Marazanye, V. T., Qadir, Z., Fahrioglu, M., & Batunlu, C. (2019). Techno-economic feasibility analysis of grid-tied PV-wind hybrid system to meet a typical household demand: Case study-Amman, Jordan. In 2019 1st Global Power, *Energy and Communication Conference* (GPECOM) (pp. 418-423). IEEE. https://doi.org/10.1109/GPECOM.2019.8778539.

Abu-Rumman, G., Khdair, A. I., & Khdair, S. I. (2020). Current status and future investment potential in renewable energy in Jordan: An overview. *Heliyon*, 6(2), e03346. https://doi.org/10.1016/j.heliyon.2020.e03346

Abu-Shikhah, N. M., Hiasat, A. A., & Al-Rabadi, W. J. (2012). A photovoltaic proposed generation promotion policy—The case of Jordan. *Energy policy*, 49, 154-163. https://doi.org/10.1016/j.enpol.2012.06.055

Adnan, S., Khan, A. H., Haider, S., & Mahmood, R. (2012). Solar energy potential in Pakistan. *Journal of Renewable and Sustainable Energy*, 4(3), 032701. https://doi.org/10.1063/1.4712051

Al Alawin, A., Badran, O., Awad, A., Abdelhadi, Y., & Al-Mofleh, A. (2012). Feasibility study of a solar chimney power plant in Jordan. *Applied Solar Energy*, 48(4), 260-265. https://doi.org/10.3103/S0003701X12040020

Al Shafeey, M., & Harb, A. M. (2018). Photovoltaic as a promising solution for peak demands and energy cost reduction in Jordan. In 2018 9th International Renewable Energy Congress (IREC) (pp. 1-4). *IEEE*. https://doi.org/10.1109/IREC.2018.8362570

Al-Addous, M., Al Hmidan, S., Jaradat, M., Alasis, E., & Barbana, N. (2020). Potential and Feasibility Study of Hybrid Wind–Hydroelectric Power System with Water-Pumping Storage: Jordan as a Case Study. *Applied Sciences*, 10(9), 3332. https://doi.org/10.3390/app10093332

Al-Addous, M., Saidan, M., Bdour, M., Dalala, Z., Albatayneh, A., & Class, C. B. (2020). Key aspects and feasibility assessment of a proposed wind farm in Jordan. *International Journal of Low-Carbon Technologies*, 15(1), 97-105. https://doi.org/10.1093/ijlct/ctz062

Alam, S., Kaushik, S. C., & Garg, S. N. (2006). Computation of beam solar radiation at normal incidence using artificial neural network. *Renewable energy*, 31(10), 1483-1491. https://doi.org/10.1016/j.renene.2005.07.010

Al-Ghriybah, M., Fadhli, Z. M., Hissein, D. D., & Mohd, S. (2019). Wind energy assessment for the capital city of Jordan, Amman. *Journal of Applied* Engineering Science, 17(3), 311-320. https://doi.org/10.5937/jaes17-20241

Al-Ghussain, L., Ahmed, H., & Haneef, F. (2018). Optimization of hybrid PV-wind system: Case study Al-Tafilah cement factory, Jordan. *Sustainable Energy Technologies and Assessments*, 30, 24-36. https://doi.org/10.1016/j.seta.2018.08.008

Al-Ghussain, L., Taylan, O., & Fahrioglu, M. (2017). Sizing of a PV-wind-oil shale hybrid system: Case analysis in Jordan. J. Sol. Energy Eng. Incl. Wind Energy Build. *Energy Conserv*. https://doi.org/10.1115/1.4038048

Alizamir, M., Kim, S., Kisi, O., & Zounemat-Kermani, M. (2020). A comparative study of several machine learning based non-linear regression methods in estimating solar radiation: Case studies of the USA and Turkey regions. *Energy*, 197, 117239. https://doi.org/10.1016/j.energy.2020.117239

Alkhalidi, A., Qoaider, L., Khashman, A., Al-Alami, A. R., & Jiryes, S. (2018). Energy and water as indicators for sustainable city site selection and design in Jordan using smart grid. *Sustainable cities and society*, 37, 125-132. https://doi.org/10.1016/j.scs.2017.10.037

Alkhalidi, A., Tahat, S., Smadi, M., Migdady, B., & Kaylani, H. (2020). Risk assessment using the analytic hierarchy process while planning and prior to constructing wind projects in Jordan. *Wind Engineering*, 44(3), 282-293. https://doi.org/10.1177/0309524X19849862

Al-Najideen, M. I., & Alrwashdeh, S. S. (2017). Design of a solar photovoltaic system to cover the electricity demand for the faculty of Engineering-Mu'tah University in Jordan. *Resource-Efficient Technologies*, 3(4), 440-445. https://doi.org/10.1016/j.reffit.2017.04.005

Al-Nhoud, O., & Al-Smairan, M. (2015). Assessment of wind energy potential as a power generation source in the Azraq South, Northeast Badia, Jordan. *Modern Mechanical Engineering*, 5(3), 87-96. https://doi.org/10.4236/mme.2015.53008

Alomari, M. H., Adeeb, J., & Younis, O. (2018). Solar photovoltaic power forecasting in jordan using artificial neural networks. *International Journal of Electrical and Computer Engineering (IJECE)*, 8(1), (497-497)PDF.

Al-omary, M., Kaltschmitt, M., & Becker, C. (2018). Electricity system in Jordan: Status & prospects. *Renewable and Sustainable Energy Reviews*, 81, 2398-2409. https://doi.org/10.1016/j.rser.2017.06.046

Alrwashdeh, S. S. (2018a). Comparison among Solar Panel Arrays Production with a Different Operating Temperatures in Amman-Jordan. *International Journal of Mechanical Engineering and Technology*, 9(6), (420-429)PDF.

Alrwashdeh, S. S. (2018b). Investigation of the energy output from PV racks based on using different tracking systems in Amman-Jordan. *Int J Mech Eng Technol*, 9, (687-690)PDF.

Alrwashdeh, S. S. (2018c). Map of Jordan governorates wind distribution and mean power density. *International Journal of Engineering & Technology*, 7(3), (1495-1500)PDF.

Alrwashdeh, S. S. (2018d). Assessment of Photovoltaic Energy Production at Different Locations in Jordan. *International Journal of Renewable Energy Research-IJRER*, 8(2)PDF.

Alrwashdeh, S. S. (2018e). Assessment of the energy production from PV racks based on using different Solar canopy form factors in Amman-Jordan. *Generations*, 5(10), (15-30)PDF.

Alrwashdeh, S. S. (2018f). The effect of solar tower height on its energy output at Ma'an-Jordan. *AIMS Energy*, 6(6), (959-966)PDF.

Alrwashdeh, S. S. (2019). Investigation of Wind Energy Production at Different Sites in Jordan Using the Site Effectiveness Method. *Energy Engineering*, 116(1), 47-59. https://doi.org/10.1080/01998595.2019.12043338

Alrwashdeh, S. S., & FMA, M. A. S. (2018). Solar radiation map of Jordan governorates. *International Journal of Engineering & Technology*, 7(3), 1664-1667. doi: 10.14419/ijet.v7i3.15557

Alsaad, M. A. (2013). Wind energy potential in selected areas in Jordan. *Energy Conversion and Management*, 65, 704-708. https://doi.org/10.1016/j.enconman.2011.12.037

Al-Salaymeh, A., Al-Hamamre, Z., Sharaf, F., & Abdelkader, M. R. (2010a). Technical and economical assessment of the utilization of photovoltaic systems in residential buildings: *The case of Jordan. Energy Conversion and Management,* 51(8), 1719-1726. https://doi.org/10.1016/j.enconman.2009.11.026

Al-Salaymeh, A., Al-Rawabdeh, I., & Emran, S. (2010b). Economical investigation of an integrated boiler–solar energy saving system in Jordan. *Energy Conversion and Management*, 51(8), 1621-1628. https://doi.org/10.1016/j.enconman.2009.08.040

Al-Sayed, R. (2013). Status of renewable energy in Jordan. In 2013 1st International Conference & Exhibition on the Applications of Information Technology to Renewable Energy Processes and Systems (pp. 66-72). *IEEE*. https://doi.org/10.1109/IT-DREPS.2013.6588153

Al-Smairan, M., & Al-Nhoud, O. (2019). Feasibility Study to Install Wind Farm in Bab Al-Hawa, Irbid, Northwest of Jordan. *Modern Mechanical Engineering*, 9(1), 30-48. https://doi.org/10.4236/mme.2019.91004

Al-Soud, M. S., & Alsafasfeh, Q. H. (2015). Economical evaluation for various renewable energy products in Jordan. In IREC2015 The Sixth International Renewable Energy Congress (pp. 1-4). *IEEE*. . https://doi.org/10.1109/IREC.2015.7110970.

Altarawneh, I. S., Rawadieh, S. I., Tarawneh, M. S., Alrowwad, S. M., & Rimawi, F. (2016). Optimal tilt angle trajectory for maximizing solar energy potential in Ma'an area in Jordan. *Journal of Renewable and Sustainable Energy*, 8(3), 033701. https://doi.org/10.1063/1.4948389

Alzoubi, H. H., & Alshboul, A. A. (2010). Low energy architecture and solar rights: Restructuring urban regulations, view from Jordan. *Renewable Energy*, 35(2), 333-342. https://doi.org/10.1016/j.renene.2009.06.017

Ammari, H. D., Al-Rwashdeh, S. S., & Al-Najideen, M. I. (2015). Evaluation of wind energy potential and electricity generation at five locations in Jordan. *Sustainable Cities and Society*, 15, 135-143. https://doi.org/10.1016/j.scs.2014.11.005

An, J., Yan, D., Guo, S., Gao, Y., Peng, J., & Hong, T. (2020). An improved method for direct incident solar radiation calculation from hourly solar insolation data in building energy simulation. *Energy and Buildings*, 227, 110425. https://doi.org/10.1016/j.enbuild.2020.110425

Anagreh, Y., & Bataineh, A. (2011). Renewable energy potential assessment in Jordan. *Renewable and Sustainable Energy Reviews*, 15(5), 2232-2239. https://doi.org/10.1016/j.rser.2011.02.010

Anagreh, Y., Bataineh, A., & Al-Odat, M. (2010). Assessment of renewable energy potential, at Aqaba in Jordan. *Renewable and sustainable energy reviews*, 14(4), 1347-1351. https://doi.org/10.1016/j.rser.2009.12.007

Arreyndip, N. A., & Joseph, E. (2018). Small 500 kW onshore wind farm project in Kribi, Cameroon: Sizing and checkers layout optimization model. *Energy Reports*, 4, 528-535. https://doi.org/10.1016/j.egyr.2018.08.003

Ayadi, O., Al-Assad, R., & Al Asfar, J. (2018). Techno-economic assessment of a grid connected photovoltaic system for the University of Jordan. *Sustainable cities and society*, 39, 93-98. https://doi.org/10.1016/j.scs.2018.02.011

Azadeh, A., Maghsoudi, A., & Sohrabkhani, S. (2009). An integrated artificial neural networks approach for predicting global radiation. *Energy conversion and management*, *50*(6), 1497-1505. https://doi.org/10.1016/j.enconman.2009.02.019

Badran, O., Abdulhadi, E., & Mamlook, R. (2010). Evaluation of solar electric power technologies in Jordan. *JJMIE*, 4(1). https://doi.org/10.1115/ES2008-54134

Baniyounes, A. M. (2017). Renewable energy potential in Jordan. *Int. J. Appl. Eng. Res*, 12(19), 8323-8331. . (8323-8331)PDF

Bataineh, A., Alqudah, A., & Athamneh, A. (2014). Optimal design of hybrid power generation system to ensure reliable power supply to the health center at Umm Jamal, Mafraq, Jordan. *Energy and Environment Research*, 4(3), 9.PDF

Benghanem, M., Mellit, A., & Alamri, S. N. (2009). ANN-based modelling and estimation of daily global solar radiation data: A case study. *Energy conversion and management*, 50(7), 1644-1655. https://doi.org/10.1016/j.enconman.2009.03.035

Bosch, J. L., Lopez, G., & Batlles, F. J. (2008). Daily solar irradiation estimation over a mountainous area using artificial neural networks. *Renewable Energy*, 33(7), 1622-1628. https://doi.org/10.1016/j.renene.2007.09.012

Boubaker, S., Kamel, S., & Kchaou, M. (2020). Prediction of Daily Global Solar Radiation using Resilient-propagation Artificial Neural Network and Historical Data: A Case Study of Hail, Saudi Arabia. *Engineering, Technology & Applied Science Research*, 10(1), 5228-5232. (5228-5232)PDF

Dalabeeh, A. S. K. (2017). Techno-economic analysis of wind power generation for selected locations in Jordan. *Renewable Energy*, 101, 1369-1378. https://doi.org/10.1016/j.renene.2016.10.003

Demircan, C., Bayrakçı, H. C., & Keçebaş, A. (2020). Machine learning-based improvement of empiric models for an accurate estimating process of global solar radiation. *Sustainable Energy Technologies and Assessments*, *37*, 100574. https://doi.org/10.1016/j.seta.2019.100574

Egeonu, D. I., Njoku, H. O., Okolo, P. N., & Enibe, S. O. (2015). Comparative assessment of temperature based ANN and Angstrom type models for predicting global solar radiation. In Afro-European conference for industrial advancement (pp. 109-122). *Springer*, Cham. https://doi.org/10.1007/978-3-319-13572-4_9

Elminir, H. K., Areed, F. F., & Elsayed, T. S. (2005). Estimation of solar radiation components incident on Helwan site using neural networks. *Solar energy*, 79(3), 270-279. https://doi.org/10.1016/j.solener.2004.11.006

El-Tous, Y., Al-Battat, S., & Hafith, S. A. (2012). Hybrid wind-PV grid connected power station case study: Al Tafila, Jordan. Int. *J. Energy Environ*, 3(4), 605-616.

Enongene, K. E., Abanda, F. H., Otene, I. J. J., Obi, S. I., & Okafor, C. (2019). The potential of solar photovoltaic systems for residential homes in Lagos city of Nigeria. *Journal of environmental management*, 244, 247-256. https://doi.org/10.1016/j.jenvman.2019.04.039

Fadare, D. A. (2009). Modelling of solar energy potential in Nigeria using an artificial neural network model. *Applied energy*, 86(9), 1410-1422. https://doi.org/10.1016/j.apenergy.2008.12.005

Fasfous, A., Asfar, J., Al-Salaymeh, A., Sakhrieh, A., Al_hamamre, Z., Al-Bawwab, A., & Hamdan, M. (2013). Potential of utilizing solar cooling in The University of Jordan. *Energy conversion and management*, 65, 729-735. https://doi.org/10.1016/j.enconman.2012.01.045

Gökçekuş, H., Kassem, Y., & Aljamal, J. (2020). Analysis of different combinations of meteorological parameters in predicting rainfall with an ANN approach: a case study in Morphou, Northern Cyprus. *Desalination and Water Treatment*, 177, 350-362.https://doi.org/10.5004/dwt.2020.24988

Guermoui, M., Melgani, F., Gairaa, K., & Mekhalfi, M. L. (2020). A comprehensive review of hybrid models for solar radiation forecasting. *Journal of Cleaner Production*, 258, 120357. https://doi.org/10.1016/j.jclepro.2020.120357

Guijo-Rubio, D., Durán-Rosal, A. M., Gutiérrez, P. A., Gómez-Orellana, A. M., Casanova-Mateo, C., Sanz-Justo, J., ... & Hervás-Martínez, C. (2020). Evolutionary artificial neural networks for accurate solar radiation prediction. Energy, 210, 118374. https://doi.org/10.1016/j.energy.2020.118374

Hammad, B., Al–Abed, M., Al–Ghandoor, A., Al–Sardeah, A., & Al–Bashir, A. (2018). Modeling and analysis of dust and temperature effects on photovoltaic systems' performance and optimal cleaning frequency: Jordan case study. *Renewable and Sustainable Energy Reviews*, 82, 2218-2234. https://doi.org/10.1016/j.rser.2017.08.070

Hasni, A., Sehli, A., Draoui, B., Bassou, A., & Amieur, B. (2012). Estimating global solar radiation using artificial neural network and climate data in the south-western region of Algeria. *Energy Procedia*, *18*, 531-537. https://doi.org/10.1016/j.egypro.2012.05.064

Hedayat, A., Davilu, H., Barfrosh, A. A., & Sepanloo, K. (2009). Estimation of research reactor core parameters using cascade feed forward artificial neural networks. *Progress in Nuclear Energy*, 51(6-7), 709-718. https://doi.org/10.1016/j.pnucene.2009.03.004

Hosseini, S. A., Kermani, A. M., & Arabhosseini, A. (2019). Experimental study of the dew formation effect on the performance of photovoltaic modules. *Renewable Energy*, 130, 352-359. https://doi.org/10.1016/j.renene.2018.06.063

Jaber, J. O., Awad, W., Rahmeh, T. A., Alawin, A. A., Al-Lubani, S., Dalu, S. A. & Al-Bashir, A. (2017). Renewable energy education in faculties of engineering in Jordan: Relationship between demographics and level of knowledge of senior students'. *Renewable and Sustainable Energy Reviews*, 73, 452-459. https://doi.org/10.1016/j.rser.2017.01.141

Jaber, J. O., Elkarmi, F., Alasis, E., & Kostas, A. (2015). Employment of renewable energy in Jordan: Current status, SWOT and problem analysis. *Renewable and Sustainable Energy Reviews*, 49, 490-499. https://doi.org/10.1016/j.rser.2015.04.050

Jiang, Y. (2008). Prediction of monthly mean daily diffuse solar radiation using artificial neural networks and comparison with other empirical models. *Energy policy*, 36(10), 3833-3837. https://doi.org/10.1016/j.enpol.2008.06.030

Jiang, Y. (2009). Computation of monthly mean daily global solar radiation in China using artificial neural networks and comparison with other empirical models. *Energy*, 34(9), 1276-1283. https://doi.org/10.1016/j.energy.2009.05.009

Kassem, Y. Azoubi, R., & Gökçekuş, H. (2019). The Possibility of Generating Electricity Using Small-Scale Wind Turbines and Solar Photovoltaic Systems for Households in Northern Cyprus: *A Comparative Study. Environments*, 6(4), 47. doi:10.3390/environments6040047 https://doi.org/10.3390/environments6040047

Kassem, Y. Gökçekuş, H., & Çamur, H. (2018). Economic assessment of renewable power generation based on wind speed and solar radiation in urban regions. Global J. Environ. Sci. Manage., 4(4), 465-482.

Kassem, Y., & Gokcekus, H. (2021). Do quadratic and Poisson regression models help to predict monthly rainfall?. Desalination and Water Treatment, 215, 288-318.

Kassem, Y., Gökçekuş, H., & Çamur, H. (2018). Wind Speed Prediction of Four Regions in Northern Cyprus Prediction Using ARIMA and Artificial Neural Networks Models: A Comparison Study. *13th International Conference on Theory and Application of Fuzzy Systems and Soft Computing — ICAFS-2018 Advances in Intelligent Systems and Computing,* 230-238. doi:10.1007/978-3-030-04164-9_32

Kassem, Y., Gökçekuş, H., & Çamur, H. (2019). Artificial Neural Networks for Predicting the Electrical Power of a New Configuration of Savonius Rotor. *Advances in Intelligent Systems and Computing 10th International Conference on Theory and Application of Soft Computing, Computing with Words and Perceptions - ICSCCW-2019,* 872-879. doi:10.1007/978-3-030-35249-3_116

Keat, S. C., Chun, B. B., San, L. H., & Jafri, M. Z. (2015). Multiple regression analysis in modelling of carbon dioxide emissions by energy consumption use in Malaysia. doi:10.1063/1.4915185

Khandelwal, A., & Shrivastava, V. (2017). Viability of grid-connected solar PV system for a village of Rajasthan. In 2017 International Conference on Information, Communication, Instrumentation and Control (ICICIC) (pp. 1-6). *IEEE*. https://doi.org/10.1109/ICOMICON.2017.8279175.

Khasawneh, Q. A., Damra, Q. A., & Bany Salman, O. H. (2015). Determining the Optimum Tilt Angle for Solar Applications in Northern Jordan. *Jordan Journal of Mechanical & Industrial Engineering*, 9(3). (187-193)PDF

Khatib, T., Mohamed, A., Mahmoud, M., & Sopian, K. (2011). Modeling of daily solar energy on a horizontal surface for five main sites in Malaysia. *International Journal of Green Energy*, 8(8), 795-819. https://doi.org/10.1080/15435075.2011.602156

Khatib, T., Mohamed, A., Sopian, K., & Mahmoud, M. (2012). Solar energy prediction for Malaysia using artificial neural networks. *International Journal of Photoenergy*, 2012. https://doi.org/10.1155/2012/419504

Koca, A., Oztop, H. F., Varol, Y., & Koca, G. O. (2011). Estimation of solar radiation using artificial neural networks with different input parameters for Mediterranean region of Anatolia in Turkey. *Expert Systems with Applications*, 38(7), 8756-8762. https://doi.org/10.1016/j.eswa.2011.01.085

Kosovic, I. N., Mastelic, T., & Ivankovic, D. (2020). Using Artificial Intelligence on environmental data from Internet of Things for estimating solar radiation: Comprehensive analysis. *Journal of Cleaner Production*, 266, 121489. https://doi.org/10.1016/j.jclepro.2020.121489

Linares-Rodríguez, A., Ruiz-Arias, J. A., Pozo-Vázquez, D., & Tovar-Pescador, J. (2011). Generation of synthetic daily global solar radiation data based on ERA-Interim reanalysis and artificial neural networks. *Energy*, 36(8), 5356-5365. https://doi.org/10.1016/j.energy.2011.06.044

Liu, H., Mi, X. W., & Li, Y. F. (2018). Wind speed forecasting method based on deep learning strategy using empirical wavelet transform, long short term memory neural network and Elman neural network. *Energy conversion and management*, *156*, 498-514. https://doi.org/10.1016/j.enconman.2017.11.053

Livingstone, D. J. (2009). Artificial neural networks (Vol. 458). *Springer*.

Lopes, F. M., Conceição, R., Fasquelle, T., Silva, H. G., Salgado, R., Canhoto, P., & Collares-Pereira, M. (2020). Predicted direct solar radiation (ECMWF) for optimized operational strategies of linear focus parabolic-trough systems. *Renewable Energy*, 151, 378-391. https://doi.org/10.1016/j.renene.2019.11.020

Meenal, R., & Selvakumar, A. I. (2018). Assessment of SVM, empirical and ANN based solar radiation prediction models with most influencing input parameters. *Renewable Energy*, *121*, 324-343. https://doi.org/10.1016/j.renene.2017.12.005

Mehmood, A., Shaikh, F. A., & Waqas, A. (2014). Modeling of the solar photovoltaic systems to fulfill the energy demand of the domestic sector of Pakistan using RETSCREEN software. In 2014 International Conference and Utility Exhibition on Green Energy for Sustainable Development (ICUE) (pp. 1-7). *IEEE*.

Mohammadi, K., Shamshirband, S., Kamsin, A., Lai, P. C., & Mansor, Z. (2016). Identifying the most significant input parameters for predicting global solar radiation using an ANFIS selection procedure. *Renewable and Sustainable Energy Reviews*, *63*, 423-434. https://doi.org/10.1016/j.rser.2016.05.065

Mubiru, J., & Banda, E. J. K. B. (2008). Estimation of monthly average daily global solar irradiation using artificial neural networks. *Solar energy*, 82(2), 181-187. https://doi.org/10.1016/j.solener.2007.06.003

Ogliari, E., Dolara, A., Manzolini, G., & Leva, S. (2017). Physical and hybrid methods comparison for the day ahead PV output power forecast. *Renewable Energy*, 113, 11-21. https://doi.org/10.1016/j.renene.2017.05.063

Okonkwo, E. C., Okwose, C. F., & Abbasoglu, S. (2017). Techno-economic analysis of the potential utilization of a hybrid PV-wind turbine system for commercial buildings in Jordan. *Int J Renew Energy Res*, 7(2), 908-914.PDF

Pastor, R., Tobarra, L., Robles-Gómez, A., Cano, J., Hammad, B., Al-Zoubi, A. & Castro, M. (2020). Renewable energy remote online laboratories in Jordan universities: Tools for training students in Jordan. *Renewable Energy*, 149, 749-759. https://doi.org/10.1016/j.renene.2019.12.100

Pham, B. T., Shirzadi, A., Bui, D. T., Prakash, I., & Dholakia, M. B. (2018). A hybrid machine learning ensemble approach based on a radial basis function neural network and rotation forest for landslide susceptibility modeling: A case study in the Himalayan area, India. *International Journal of Sediment Research*, 33(2), 157-170. https://doi.org/10.1016/j.ijsrc.2017.09.008

Polo, J., Fernández-Peruchena, C., Salamalikis, V., Mazorra-Aguiar, L., Turpin, M., Martín-Pomares, L & Remund, J. (2020). Benchmarking on improvement and site-adaptation techniques for modeled solar radiation datasets. *Solar Energy*, 201, 469-479. https://doi.org/10.1016/j.solener.2020.03.040

Premalatha, M., & Naveen, C. (2018). Analysis of different combinations of meteorological parameters in predicting the horizontal global solar radiation with ANN approach: A case study. *Renewable and Sustainable Energy Reviews*, *91*, 248-258. https://doi.org/10.1016/j.rser.2018.03.096

Qasaimeh, A., Qasaimeh, M., Abu-Salem, Z., & Momani, M. (2014). Solar Energy Sustainability in Jordan. Computational Water, Energy, *and Environmental Engineering*, 2014. https://doi.org/10.4236/cweee.2014.32006

Rahimikhoob, A. (2010). Estimating global solar radiation using artificial neural network and air temperature data in a semi-arid environment. *Renewable Energy*, *35*(9), 2131-2135. https://doi.org/10.1016/j.renene.2010.01.029

Rezrazi, A., Hanini, S., & Laidi, M. (2016). An optimisation methodology of artificial neural network models for predicting solar radiation: a case study. *Theoretical and applied climatology*, 123(3-4), 769-783. https://doi.org/10.1007/s00704-015-1398-x

Riahi, K., Vuuren, D. P., Kriegler, E., Edmonds, J., O'Neill, B. C., Fujimori, S,Tavoni, M. (2017). The Shared Socioeconomic Pathways and their energy, land use, and greenhouse gas emissions implications: An overview. *Global Environmental Change*, 42, 153-168. https://doi.org/10.1016/j.gloenvcha.2016.05.009

Rumbayan, M., Abudureyimu, A., & Nagasaka, K. (2012). Mapping of solar energy potential in Indonesia using artificial neural network and geographical information system. *Renewable and Sustainable Energy Reviews*, *16*(3), 1437-1449. https://doi.org/10.1016/j.rser.2011.11.024

Safaripour, M. H., & Mehrabian, M. A. (2011). Predicting the direct, diffuse, and global solar radiation on a horizontal surface and comparing with real data. Heat and mass transfer, 47(12), 1537-1551. https://doi.org/10.1007/s00231-011-0814-8

Sakhrieh, A., & Al-Ghandoor, A. (2013). Experimental investigation of the performance of five types of solar collectors. *Energy Conversion and Management*, 65, 715-720. https://doi.org/10.1016/j.enconman.2011.12.038

Schnitzer, H., Brunner, C., & Gwehenberger, G. (2007). Minimizing greenhouse gas emissions through the application of solar thermal energy in industrial processes. *Journal of Cleaner Production*, 15(13-14), 1271-1286. doi:10.1016/j.jclepro.2006.07.023

Şenkal, O., & Kuleli, T. (2009). Estimation of solar radiation over Turkey using artificial neural network and satellite data. *Applied energy*, 86(7-8), 1222-1228. https://doi.org/10.1016/j.apenergy.2008.06.003

Shahsavari, A., & Akbari, M. (2018). Potential of solar energy in developing countries for reducing energy-related emissions. *Renewable and Sustainable Energy Reviews*, 90, 275-291. doi:10.1016/j.rser.2018.03.065

Shahsavari, A., Yazdi, F. T., & Yazdi, H. T. (2018). Potential of solar energy in Iran for carbon dioxide mitigation. *International Journal of Environmental Science and Technology*, 16(1), 507-524. doi:10.1007/s13762-018-1779-7

Simsek, E., Williams, M. J., & Pilon, L. (2021). Effect of dew and rain on photovoltaic solar cell performances. *Solar Energy Materials and Solar Cells*, 222, 110908. https://doi.org/10.1016/j.solmat.2020.110908

Tashtoush, B., Alshare, A., & Al-Rifai, S. (2015). Hourly dynamic simulation of solar ejector cooling system using TRNSYS for Jordanian climate. *Energy conversion and management*, 100, 288-299. https://doi.org/10.1016/j.enconman.2015.05.010

Tymvios, F. S., Jacovides, C. P., Michaelides, S. C., & Scouteli, C. (2005). Comparative study of Ångström's and artificial neural networks' methodologies in estimating global solar radiation. *Solar energy*, 78(6), 752-762. https://doi.org/10.1016/j.solener.2004.09.007

Vijayavenkataraman, S., Iniyan, S., & Goic, R. (2012). A review of climate change, mitigation, and adaptation. *Renewable and Sustainable Energy Reviews*, 16(1), 878-897. https://doi.org/10.1016/j.rser.2011.09.009.

Worki, Y., Berhan, E., & Krejcar, O. (2016, September). Global Solar Radiation Prediction Using Backward Propagation Artificial Neural Network for the City of Addis Ababa, Ethiopia. In International Conference on Computational Collective Intelligence (pp. 230-238). *Springer*, Cham. https://doi.org/10.1007/978-3-319-45243-2_21

Yadav, A. K., Malik, H., & Chandel, S. S. (2014). Selection of most relevant input parameters using WEKA for artificial neural network based solar radiation prediction models. *Renewable and Sustainable Energy Reviews*, *31*, 509-519. https://doi.org/10.1016/j.rser.2013.12.008

Yesilata, B., & Firatoglu, Z. A. (2008). Effect of solar radiation correlations on system sizing: PV pumping case. *Renewable Energy*, 33(1), 155-161. https://doi.org/10.1016/j.renene.2007.01.005

Yildiz, B. Y., Şahin, M., Şenkal, O. Z. A. N., Pestemalci, V. E. D. A. T., & Emrahoğlu, N. (2013). A comparison of two solar radiation models using artificial neural networks and remote sensing in Turkey. *Energy Sources, Part A: Recovery, Utilization, and Environmental Effects*, *35*(3), 209-217. https://doi.org/10.1080/15567036.2011.650276

Yu, C., Li, Y., & Zhang, M. (2017). Comparative study on three new hybrid models using Elman Neural Network and Empirical Mode Decomposition based technologies improved by Singular Spectrum Analysis for hour-ahead wind speed forecasting. *Energy Conversion and Management*, 147, 75-85. https://doi.org/10.1016/j.enconman.2017.05.008

Yu, D., Wang, Y., Liu, H., Jermsittiparsert, K., & Razmjooy, N. (2019). System identification of PEM fuel cells using an improved Elman neural network and a new hybrid optimization algorithm. *Energy Reports*, 5, 1365-1374. https://doi.org/10.1016/j.egyr.2019.09.039

Zheng, Y., Shadloo, M. S., Nasiri, H., Maleki, A., Karimipour, A., & Tlili, I. (2020). Prediction of viscosity of biodiesel blends using various artificial model and comparison with empirical correlations. *Renewable Energy*, 153, 1296-1306.https://doi.org/10.1016/j.renene.2020.02.087

Zyadin, A., Puhakka, A., Ahponen, P., Cronberg, T., & Pelkonen, P. (2012). School students' knowledge, perceptions, and attitudes toward renewable energy in Jordan. *Renewable energy*, 45, 78-85. https://doi.org/10.1016/j.renene.2012.02.002

Appendices

Appendix A

Performance of the proposed models

Table 4.2

Performance of the proposed models with one input

Model	Variable	HL	NN	TF	MSE	R^2	RMSE
			MFFNN				
MFFNN#1	D	1	5	TAN	4.26E-05	0.0028	0.1197
MFFNN#2	Ta	1	5	TAN	2.81E-05	0.1088	0.0089
MFFNN#3	Tmax	1	5	TAN	4.12E-05	0.0148	0.0150
MFFNN#4	Tmin	1	5	TAN	4.03E-05	0.1616	0.0067
MFFNN#5	Tw	1	5	LOG	4.94E-05	0.0000	0.0114
MFFNN#6	GSR	1	5	LOG	3.72E-05	0.0556	0.1208
MFFNN#7	WS	1	5	LOG	9.86E-06	0.0558	**0.0024**
MFFNN#8	RH	1	5	TAN	0.000137	0.0232	0.0064
			CFNN				
CFNN#1	D	1	5	LOG	3.94E-05	0.0094	0.0754
CFNN#2	Ta	1	5	LOG	2.76E-05	0.0026	0.2514
CFNN#3	Tmax	1	5	TAN	3.67E-05	0.0140	0.0129
CFNN#4	Tmin	1	5	LOG	0.023369	0.0025	0.0251
CFNN#5	Tw	1	5	TAN	0.000162	0.0039	0.0112
CFNN#6	GSR	1	5	TAN	4.16E-05	0.0193	0.0764
CFNN#7	WS	1	5	TAN	9.69E-05	0.0118	0.0099
CFNN#8	RH	1	5	LOG	2.63E-05	0.0004	0.0114
			ENN				
ENN#1	D	1	5	TAN	4.26E-05	0.0028	0.1197
ENN#2	Ta	1	5	TAN	3.58E-06	0.2549	**0.0021**
ENNl#3	Tmax	1	5	TAN	1.35E-05	0.0051	0.0032
ENN#4	Tmin	1	8	LOG	3.87E-05	0.0000	0.0070
ENN#5	Tw	1	5	TAN	8.87E-06	0.1614	0.0029
ENN#6	GSR	1	5	TAN	3.92E-05	**0.4565**	0.1208
ENN#7	WS	1	5	LOG	2.11E-05	0.0104	0.0036
ENN#8	RH	1	5	TAN	2.72E-05	0.0110	0.1456
			RBFNN				
RBFNN#1	D	-	2	-	0.005051	0.4314	0.0074
RBFNN#2	Ta	-	2	-	0.00506	0.1007	0.0080
RBFNN#3	Tmax	-	2	-	0.005065	0.2005	0.0075
RBFNN#4	Tmin	-	2	-	0.005058	0.0401	0.0080
RBFNN#5	Tw	-	2	-	0.005072	0.0009	0.0068
RBFNN#6	GSR	-	2	-	0.00501	**0.8472**	0.0136
RBFNN#7	WS	-	2	-	0.005073	0.0480	0.0073
RBFNN#8	RH	-	2	-	0.005053	0.3936	0.0082

Table 4.3

Performance of the proposed models with two inputs

Model	Variable	HL	NN	TF	MSE	R^2	RMSE
			MFFNN				
MFFNN#9	Ta,Tmax	1	5	TAN	4.03E-05	0.1277	0.0070
MFFNN#10	Ta,Tmin	1	8	LOG	7.06E-06	0.0884	0.0179
MFFNN#11	Ta,Tw	1	5	TAN	0.033544	0.2124	0.0166
MFFNN#12	Ta,GSR	1	8	LOG	6.83E-06	0.0360	0.0751
MFFNN#13	Ta,WS	1	5	TAN	3.04E-05	0.0121	0.0867
MFFNN#14	Ta,RH	1	5	TAN	3.0799-06	0.0342	0.0040
MFFNN#15	Tmax,Tmin	1	5	LOG	4E-05	0.0239	0.0064
MFFNN#16	Tmax,Ta	1	5	TAN	1.52E-05	0.0014	0.0048
MFFNN#17	Tmax,Tw	1	5	TAN	1.54E-06	0.0107	0.0334
MFFNN#18	Tmax,WS	1	5	LOG	1.59E-05	0.0835	0.0409
MFFNN#19	Tmax,RH	1	5	TAN	5.47E-06	0.2163	0.0022
MFFNN#20	Tmin,Tw	1	5	LOG	5.77E-05	0.1312	0.0074
MFFNN#21	Tmin,GSR	1	5	TAN	8.41E-06	0.2052	0.0030
MFFNN#22	Tmin,WS	1	5	LOG	1.61E-05	0.0048	0.0170
MFFNN#23	Tmin,RH	1	5	TAN	2.66E-06	0.0272	0.0730
MFFNN#24	Tw,GSR	1	5	TAN	4.28E-06	0.0081	0.1037
MFFNN#25	Tw,WS	1	8	LOG	3.85E-05	0.0021	0.1043
MFFNN#26	Tw,RH	1	5	TAN	1.78E-05	0.0016	0.0064
MFFNN#27	GSR,WS	1	5	LOG	1.6E-05	0.0355	0.0812
MFFNN#28	GSR,RH	1	5	LOG	3.33E-05	0.0073	0.0262
MFFNN#29	WS,RH	1	5	TAN	1.55E-05	0.0365	0.0044
MFFNN#30	D,Ta	1	5	TAN	5.34E-05	0.0366	0.0065
MFFNN#31	D,Tmax	1	5	TAN	3.92E-05	0.0060	0.0644
MFFNN#32	D,Tmin	1	5	TAN	5.11E-05	0.0028	0.0067
MFFNN#33	D,Tw	1	5	TAN	6.51E-06	0.0556	0.1030
MFFNN#34	D,GSR	1	8	LOG	9E-05	0.0125	0.0540
MFFNN#35	D,Ws	1	5	TAN	1.74E-05	0.1343	0.0041
MFFNN#36	D,RH	1	5	LOG	0.00013	0.0035	0.0064
			CFNN				
CFNN#9	Ta,Tmax	1	5	LOG	7E-06	0.0211	0.1435
CFNN#10	Ta,Tmin	1	5	TAN	9.76E-06	0.0306	0.1521
CFNN#11	Ta,Tw	1	5	TAN	0.00055	0.0260	0.0209
CFNN#12	Ta,GSR	1	5	LOG	8.87E-05	0.8524	0.0010
CFNN#13	Ta,WS	1	5	TAN	6.56E-05	0.0151	0.1170
CFNN#14	Ta,RH	1	5	TAN	2.96E-06	0.5053	0.0016

Table**.** 4.3 **(**Continued).

Model	Variable	HL	NN	TF	MSE	R^2	RMSE
			CFNN				
CFNN#15	Tmax,Tmin	1	5	LOG	0.000504	0.1299	0.0258
CFNN#16	Tmax,Ta	1	5	TAN	3.35E-05	0.0015	0.0140
CFNN#17	Tmax,Tw	1	8	LOG	2.22E-05	0.0367	0.1681
CFNN#18	Tmax,WS	1	5	TAN	8.24E-05	0.0102	0.0087
CFNN#19	Tmax,RH	1	5	LOG	1.89E-05	0.0032	0.0287
CFNN#20	Tmin,Tw	1	8	LOG	6.1E-05	0.0003	0.1419
CFNN#21	Tmin,GSR	1	5	LOG	2.27E-05	0.0682	0.0057
CFNN#22	Tmin,WS	1	5	LOG	8.06E-05	0.0084	0.0096
CFNN#23	Tmin,RH	1	8	LOG	7.08E-06	0.0114	0.2010
CFNN#24	Tw,GSR	1	5	LOG	3.19E-05	0.3652	0.0067
CFNN#25	Tw,WS	1	5	TAN	2.44E-05	0.0085	0.0066
CFNN#26	Tw,RH	1	8	LOG	5.14E-05	0.0391	0.0116
CFNN#27	GSR,WS	1	5	LOG	9.44E-05	0.6907	0.0098
CFNN#28	GSR,RH	1	8	LOG	1.19E-06	0.0235	0.1469
CFNN#29	WS,RH	1	5	TAN	0.000153	0.1158	0.0106
CFNN#30	D,Ta	1	5	LOG	0.000487	0.2980	0.0232
CFNN#31	D,Tmax	1	5	TAN	1.79E-05	0.0633	0.0046
CFNN#32	D,Tmin	1	5	LOG	4.1E-05	0.0200	0.1774
CFNN#33	D,Tw	1	5	LOG	7.69E-06	0.0123	0.1470
CFNN#34	D,GSR	1	5	TAN	3.16E-05	0.1564	0.0094
CFNN#35	D,Ws	1	5	LOG	4.04E-05	0.0555	0.0070
CFNN#36	D,RH	1	5	TAN	0.009976	0.0171	0.0054
			ENN				
ENN#9	Ta,Tmax	1	5	TAN	0.000132	0.0113	0.0049
ENN#10	Ta,Tmin	1	5	LOG	3.54E-05	0.0393	0.0070
ENN#11	Ta,Tw	1	5	LOG	3.59E-05	0.0239	0.0070
ENN#12	Ta,GSR	1	5	LOG	8.28E-06	0.0056	0.1410
ENN#13	Ta,WS	1	5	LOG	2.28E-05	0.0027	0.1808
ENN#14	Ta,RH	1	8	LOG	2.96E-05	0.3165	0.0051
ENN#15	Tmax,Tmin	1	5	LOG	4.66E-05	0.0224	0.0070
ENN#16	Tmax,Ta	1	5	TAN	2.13E-05	0.0921	0.0049
ENN#17	Tmax,Tw	1	5	LOG	8.7E-06	0.1098	0.0029
ENN#18	Tmax,WS	1	5	LOG	0.000158	0.0109	0.0721
ENN#19	Tmax,RH	1	5	LOG	2.45E-05	0.1036	0.0056
ENN#20	Tmin,Tw	1	5	LOG	1.16E-05	0.1589	0.0033
ENN#21	Tmin,GSR	1	5	TAN	3.41E-05	0.0395	0.0058

Table 4.3 **(**Continued).

Model	Variable	HL	NN	TF	MSE	R^2	RMSE
			ENN				
ENN#22	Tmin,WS	1	5	TAN	1.56E-05	0.0025	0.1288
ENN#23	Tmin,RH	1	5	TAN	0.000227	0.0245	0.0153
ENN#24	Tw,GSR	1	5	LOG	6.84E-07	**0.9090**	**0.0007**
ENN#25	Tw,WS	1	5	TAN	0.02359	0.0026	0.0280
ENN#26	Tw,RH	1	5	TAN	4.96E-06	0.2952	0.0027
ENN#27	GSR,WS	1	8	LOG	1.93E-05	0.2528	0.0051
ENN#28	GSR,RH	1	5	LOG	4.4E-05	0.7355	0.0072
ENN#29	WS,RH	1	5	TAN	0.010329	0.0594	0.0050
ENN#30	D,Ta	1	5	LOG	1.31E-05	0.0366	0.0065
ENN#31	D,Tmax	1	5	TAN	8.06E-06	0.5120	0.0017
ENN#32	D,Tmin	1	5	TAN	5.39E-05	0.0028	0.0067
ENN#33	D,Tw	1	5	LOG	7.32E-06	0.1605	0.0023
ENN#34	D,GSR	1	5	TAN	2.61E-05	0.0340	0.0043
ENN#35	D,Ws	1	5	LOG	1.93E-05	0.0113	0.1202
ENN#36	D,RH	1	5	TAN	0.000283	0.1411	0.0200
			RBFNN				
RBFNN#9	Ta,Tmax	-	2	-	0.005065	0.1474	0.0076
RBFNN#10	Ta,Tmin	-	2	-	0.004997	0.2587	0.0127
RBFNN#11	Ta,Tw	-	2	-	0.005043	0.0021	0.0098
RBFNN#12	Ta,GSR	-	2	-	0.004996	0.6991	0.0092
RBFNN#13	Ta,WS	-	2	-	0.005076	0.1839	0.0069
RBFNN#14	Ta,RH	-	2	-	0.00507	0.2505	0.0074
RBFNN#15	Tmax,Tmin	-	2	-	0.004986	0.2286	0.0127
RBFNN#16	Tmax,Ta	-	2	-	0.005031	0.3069	0.0105
RBFNN#17	Tmax,Tw	-	2	-	0.005005	0.7591	0.0088
RBFNN#18	Tmax,WS	-	2	-	0.005068	0.3068	0.0075
RBFNN#19	Tmax,RH	-	2	-	0.005062	0.1912	0.0080
RBFNN#20	Tmin,Tw	-	2	-	0.005078	0.0733	0.0070
RBFNN#21	Tmin,GSR	-	2	-	0.005078	0.0733	0.0070
RBFNN#22	Tmin,WS	-	2	-	0.005065	0.0078	0.0074
RBFNN#23	Tmin,RH	-	2	-	0.005006	0.0723	0.0120
RBFNN#24	Tw,GSR	-	2	-	0.004978	0.4052	0.0112
RBFNN#25	Tw,WS	-	2	-	0.005058	0.0015	0.0082
RBFNN#26	Tw,RH	-	2	-	0.005003	0.0925	0.0115
RBFNN#27	GSR,WS	-	2	-	0.005003	0.2940	0.0136
RBFNN#28	GSR,RH	-	2	-	0.005019	0.8977	0.0087
RBFNN#29	WS,RH	-	2	-	0.005049	0.2589	0.0085

Table 3.4 **(**Continued).

Model	Variable	HL	NN	TF	MSE	R^2	RMSE
			RBFNN				
RBFNN#30	D,Ta	-	2	-	0.005047	0.3925	0.0072
RBFNN#31	D,Tmax	-	2	-	0.005037	0.4594	0.0079
RBFNN#32	D,Tmin	-	2	-	0.005057	0.1083	0.0066
RBFNN#33	D,Tw	-	2	-	0.004977	0.7254	0.0096
RBFNN#34	D,GSR	-	2	-	0.00504	0.0589	0.0093
RBFNN#35	D,Ws	-	2	-	0.005035	0.3133	0.0089
RBFNN#36	D,RH	-	2	-	0.005012	0.4498	0.0096

Table 4.4

Performance of the proposed models with three inputs

Model	Variable	HL	NN	TF	MSE	R^2	RMSE
			MFFNN				
MFFNN#37	D,Ta,Tmax	1	8	LOG	5.78E-06	0.2809	0.0054
MFFNN#38	D,Ta,Tmin	1	5	LOG	9.38E-05	0.0316	0.1041
MFFNN#39	D,Ta,Tw	1	5	LOG	6.24E-06	0.5072	**0.0023**
MFFNN#40	D,Ta,GSR	1	5	TAN	3.9E-06	0.3284	0.0036
MFFNN#41	D,Ta,WS	1	5	LOG	7.2E-06	0.2797	0.0042
MFFNN#42	D,Ta,RH	1	5	LOG	1.5E-05	0.3011	0.0036
			CFNN				
CFNN#37	D,Ta,Tmax	1	5	TAN	5.61E-06	0.5560	0.0016
CFNN#38	D,Ta,Tmin	1	5	TAN	3.43E-05	0.0168	0.1057
CFNN#39	D,Ta,Tw	1	5	LOG	4.11E-05	0.0243	0.1385
CFNN#40	D,Ta,GSR	1	5	LOG	3.74E-05	0.2436	0.0069
CFNN#41	D,Ta,WS	1	5	LOG	1.91E-05	0.0112	0.1044
CFNN#42	D,Ta,RH	1	5	LOG	1.5E-05	0.0394	0.1800
			ENN				
ENN#37	D,Ta,Tmax	1	8	LOG	4.7E-06	0.4746	0.0028
ENN#38	D,Ta,Tmin	1	5	LOG	5.77E-06	0.6382	0.0031
ENN#39	D,Ta,Tw	1	5	TAN	0.009939	0.2601	0.0098
ENN#40	D,Ta,GSR	1	5	LOG	8.92E-06	0.0718	0.0070
ENN#41	D,Ta,WS	1	5	TAN	1.7E-05	0.0004	0.1475
ENN#42	D,Ta,RH	1	5	TAN	1.65E-05	0.0101	0.0407
			RBFNN				
RBFNN#37	D,Ta,Tmax	-	2	-	0.005041	0.5222	0.0081
RBFNN#38	D,Ta,Tmin	-	2	-	0.005048	0.3211	0.0069
RBFNN#39	D,Ta,Tw	-	2	-	0.00502	0.2601	0.0098
RBFNN#40	D,Ta,GSR	-	2	-	0.00499	**0.7420**	0.0093
RBFNN#41	D,Ta,WS	-	2	-	0.005041	0.1451	0.0082
RBFNN#42	D,Ta,RH	-	2	-	0.005014	0.2419	0.0096

Table 4.5

Performance of the proposed models with four inputs

Model	Variable	HL	NN	TF	MSE	R^2	RMSE
			MFFNN				
MFFNN#43	D,Ta,Tmax,Tmin	1	5	TAN	2.42E-05	0.0343	0.0327
MFFNN#44	D,Ta,Tmax,Tw	1	5	LOG	5.16E-06	0.3440	**0.0026**
MFFNN#45	D,Ta,Tmax,GSR	1	5	LOG	0.000114	0.0114	0.1803
MFFNN#46	D,Ta,Tmax,WS	1	8	LOG	9.74E-05	0.0114	0.1476
MFFNN#47	D,Ta,Tmax,RH	1	5	TAN	2.91E-06	0.0733	0.0052
			CFNN				
CFNN#43	D,Ta,Tmax,Tmin	1	5	LOG	3.85E-06	0.0333	0.1225
CFNN#44	D,Ta,Tmax,Tw	1	8	LOG	1.17E-05	0.0308	0.0636
CFNN#45	D,Ta,Tmax,GSR	1	5	TAN	5.19E-06	0.0439	0.0793
CFNN#46	D,Ta,Tmax,WS	1	5	TAN	0.009555	0.3061	0.0136
CFNN#47	D,Ta,Tmax,RH	1	5	TAN	4.77E-05	0.0987	0.0106
			ENN				
ENN#43	D,Ta,Tmax,Tmin	1	8	LOG	3.14E-06	0.0162	0.1040
ENN#44	D,Ta,Tmax,Tw	1	5	LOG	0.024434	0.1535	0.0070
ENN#45	D,Ta,Tmax,GSR	1	5	LOG	9.12E-07	0.0114	0.1803
ENN#46	D,Ta,Tmax,WS	1	5	LOG	2.21E-05	**0.4583**	0.0035
ENN#47	D,Ta,Tmax,RH	1	5	TAN	2.91E-06	0.0733	0.0052
			RBFNN				
RBFNN#43	D,Ta,Tmax,Tmin	-	2	-	0.005028	0.3930	0.0082
RBFNN#44	D,Ta,Tmax,Tw	-	2	-	0.004998	0.2505	0.0105
RBFNN#45	D,Ta,Tmax,GSR	-	2	-	0.004992	**0.7796**	0.0092
RBFNN#46	D,Ta,Tmax,WS	-	2	-	0.005044	0.1139	0.0082
RBFNN#47	D,Ta,Tmax,RH	-	2	-	0.004986	0.7764	0.0096

Table 4.6

Performance of the proposed models with five inputs

Model	Variable	HL	NN	TF	MSE	R^2	RMSE
			MFFNN				
MFFNN#48	D,Ta,Tmax,Tmin,Tw	1	5	TAN	4.92E-06	0.0437	0.1144
MFFNN#49	D,Ta,Tmax,Tmin,GSR	1	5	LOG	9.58E-05	0.0219	0.0106
MFFNN#50	D,Ta,Tmax,Tmin,WS	1	5	LOG	2.71E-06	0.0954	0.0166
MFFNN#51	D,Ta,Tmax,Tmin,RH	1	5	TAN	7.36E-06	0.0083	0.1021
			CFNN				
CFNN#48	D,Ta,Tmax,Tmin,Tw	1	5	LOG	9.86E-05	0.0175	0.1811
CFNN#49	D,Ta,Tmax,Tmin,GSR	1	5	LOG	0.000771	0.2778	0.0288
CFNN#50	D,Ta,Tmax,Tmin,WS	1	5	LOG	4.51E-05	0.0634	0.0356
CFNN#51	D,Ta,Tmax,Tmin,RH	1	8	LOG	7.1E-06	0.0165	0.0906
			ENN				
ENN#48	D,Ta,Tmax,Tmin,Tw	1	5	TAN	0.009899	**0.5059**	0.0233
ENN#49	D,Ta,Tmax,Tmin,GSR	2	5	LOG	9.58E-05	0.0219	0.0106
ENN#50	D,Ta,Tmax,Tmin,WS	1	5	TAN	1.26E-05	0.0025	0.1295
ENN#51	D,Ta,Tmax,Tmin,RH	1	5	TAN	0.000447	0.3050	0.0253
			RBFNN				
RBFNN#48	D,Ta,Tmax,Tmin,Tw	-	2	-	0.005011	0.2458	0.0098
RBFNN#49	D,Ta,Tmax,Tmin,GSR	-	2	-	0.005007	0.4527	0.0100
RBFNN#50	D,Ta,Tmax,Tmin,WS	-	2	-	0.005042	0.1093	**0.0082**
RBFNN#51	D,Ta,Tmax,Tmin,RH	-	2	-	0.005005	0.3050	0.0253

Table 4.7

Performance of the proposed models with six inputs

Model	Variable	HL	NN	TF	MSE	R^2	RMSE
			MFFNN				
MFFNN#52	D,Ta,Tmax,Tmin,Tw,GSR	1	5	TAN	7.2551E-06	**0.8429**	**0.0025**
MFFNN#53	D,Ta,Tmax,Tmin,Tw,WS	1	5	LOG	0.000094107	0.3136	0.0036
MFFNN#54	D,Ta,Tmax,Tmin,Tw,RH	1	5	TAN	7.1252E-06	0.0492	0.1586
			CFNN				
CFNN#52	D,Ta,Tmax,Tmin,Tw,GSR	1	5	LOG	0.00028141	0.0983	0.0240
CFNN#53	D,Ta,Tmax,Tmin,Tw,WS	1	5	TAN	0.000018485	0.0694	0.2152
CFNN#54	D,Ta,Tmax,Tmin,Tw,RH	1	5	LOG	0.00025271	0.0858	0.0042
			ENN				
ENN#52	D,Ta,Tmax,Tmin,Tw,GSR	1	5	TAN	2.3393E-06	0.0267	0.0319
ENN#53	D,Ta,Tmax,Tmin,Tw,WS	1	5	TAN	0.000092218	0.0291	0.0263
ENN#54	D,Ta,Tmax,Tmin,Tw,RH	1	5	TAN	2.4514E-06	0.0058	0.2210
			RBFNN				
RBFNN#52	D,Ta,Tmax,Tmin,Tw,GSR	-	2	-	0.00497947	0.7165	0.0099
RBFNN#53	D,Ta,Tmax,Tmin,Tw,WS	-	2	-	0.00503192	0.0303	0.0093
RBFNN#54	D,Ta,Tmax,Tmin,Tw,RH	-	2	-	0.00500603	0.2941	0.0106

Table 4.8

Performance of the proposed models with seven inputs

Model	Variable	HL	NN	TF	MSE	R^2	RMSE
			MFFNN				
MFFNN#55	D,Ta,Tmax,Tmin,Tw,GSR, WS	1	5	LOG	2.3735E-06	0.0409	0.0448
MFFNN#56	D,Ta,Tmax,Tmin,Tw,GSR, RH	1	8	LOG	3.5354E-06	0.1070	0.0103
			CFNN				
CFNN#55	D,Ta,Tmax,Tmin,Tw,GSR, WS	1	5	TAN	0.0016807	0.2688	0.0427
CFNN#56	D,Ta,Tmax,Tmin,Tw,GSR, RH	1	5	LOG	0.00001632	0.0312	0.1037
			ENN				
ENN#55	D,Ta,Tmax,Tmin,Tw,GSR, WS	1	5	LOG	0.00024112	0.4260	0.0148
ENN#56	D,Ta,Tmax,Tmin,Tw,GSR, RH	1	5	TAN	3.9848E-07	**0.8168**	**0.0011**
			RBFNN				
RBFNN#55	D,Ta,Tmax,Tmin,Tw,GSR, WS	-	2	-	0.00497371	0.4260	0.0148
RBFNN#56	D,Ta,Tmax,Tmin,Tw,GSR, RH	-	2	-	0.00499233	0.5971	0.0103

Table 4.9

Performance of the proposed models with eight inputs

Model	Variable	HL	NN	TF	MSE	R^2	RMSE
			MFFNN				
MFFNN#57	D,Ta,Tmax,Tmin,Tw,GSR,WS,RH	1	5	LOG	0.00002917	0.0692	0.1160
			CFNN				
CFNN#57	D,Ta,Tmax,Tmin,Tw,GSR,WS,RH	1	5	LOG	9.4502E-07	**0.8623**	**0.0011**
			ENN				
ENN#57	D,Ta,Tmax,Tmin,Tw,GSR,WS,RH	1	5	LOG	0.000017782	0.0398	0.1086
			RBFNN				
RBFNN#57	D,Ta,Tmax,Tmin,Tw,GSR	-	2	-	0.00499465	0.2662	0.0113

Appendix B

Turnitin Similarity Report

All thesis

ORIGINALITY REPORT

14%	9%	12%	2%
SIMILARITY INDEX	INTERNET SOURCES	PUBLICATIONS	STUDENT PAPERS

PRIMARY SOURCES

1	Submitted to National Institute of Technology, Rourkela Student Paper	1%
2	ipbes.net Internet Source	1%
3	Pratima Kumari, Durga Toshniwal. "Deep learning models for solar irradiance forecasting: A comprehensive review", Journal of Cleaner Production, 2021 Publication	1%
4	docs.neu.edu.tr Internet Source	<1%
5	ipcc.ch Internet Source	<1%
6	Kunal Sandip Garud, Simon Jayaraj, Moo - Yeon Lee. "A review on modeling of solar photovoltaic systems using artificial neural networks, fuzzy logic, genetic algorithm and hybrid models", International Journal of Energy Research, 2020 Publication	<1%